COMPUTED TOMOGRAPHY OF THE THORAX AND ABDOMEN OF THE CLINICALLY NORMAL COMMON MARMOSET (*Callithrix jacchus*)

by

Wencke M. du Plessis

Submitted in fulfilment of the requirements
for the degree of Doctor of Philosophy (PhD)
in the Faculty of Veterinary Science, University of Pretoria

February 2015

COMPUTED TOMOGRAPHY OF THE THORAX AND ABDOMEN OF THE CLINICALLY NORMAL COMMON MARMOSET (*Callithrix jacchus*)

by

Wencke M. du Plessis

Supervisor: Prof. Hermanus B. Groenewald
Department of Anatomy and Physiology
Faculty of Veterinary Science
University of Pretoria

Co-supervisor: Prof. Lorrie Gaschen
Diagnostic Imaging, Veterinary Clinical Sciences
School of Veterinary Medicine
Louisiana State University

DECLARATION

I declare that the thesis herewith submitted by me to the University of Pretoria for the degree of PhD, has not been submitted previously by me for a degree at any other university.

Candidate: _____ _____

Wencke M. du Plessis Date

Abigail, Vincent & Albert

Dreams are there to be realized

ACKNOWLEDGEMENTS

My sincere thanks to Prof. Hermanus B. Groenewald and Prof. Lorrie Gaschen for the supervision of this dissertation. Thank you for all your support and encouragement.

Thank you also to my external examiners…since I know it is a tremendous amount of work committing to such a task, and it is highly appreciated.

Thanks also to the Exotic Animal Clinic for helping with the anaesthesia, and the radiology sisters of the Onderstepoort Veterinary Academic Hospital for technical assistance for the CT procedures.

And last but not least…to my children Abigail and Vincent and my husband Albert…for all the weekends, holidays, evenings and early mornings that you allowed me to work on this PhD. You are my strength and my sunshine…and the true reason why this PhD became reality….To infinity and beyond.

Thank you.

ABSTRACT

The aim of this study was: 1) to describe the computed tomographic thoracic and abdominal anatomy in the clinically normal common marmoset; 2) to describe the normal reference range of Hounsfield units (HU) of major abdominal and thoracic organs; 3) to refine the computed tomography (CT) protocol; 4) to compare abdominal CT to other imaging modalities such as radiography and ultrasound (US).

Eight clinically healthy mature common marmosets ranging from 12 to 48 months and 235 to 365 g bodyweight were anesthetised and pre- and post-contrast CT examinations were performed using different CT settings. In 3/8 common marmosets radiography was performed at the same time.

Diagnostic quality images could be obtained in the common marmoset despite its small size and high respiration rate using a dual slice CT scanner. Quantitative and qualitative assessments of major thoracic and abdominal structures were obtained. The HU of major abdominal and thoracic organs differed from small animals. Representative cross-sectional images were selected and relevant anatomy was labeled. None of the thoracic lymph nodes were detected and separation of individual lung lobes – besides the accessory – was only occasionally seen. Identification and delineation of abdominal organs greatly improved with i.v. contrast. A high frequency algorithm with edge enhancement proved to be particularly beneficial for the evaluation of thoracic and to a lesser degree abdominal CT. Due to their size and species specific anatomy (also reflected in their different normal range of HU of individual organs), standard small animal CT protocols need to be critically assessed and adapted for exotics, such as the

common marmosets. Imaging findings differed from described anatomic findings (such as positioning of kidneys in relationship to lumbar vertebrae) and could either be due to different study population, imply more mobility of kidneys similar to cats, or emphasize that CT might be better for certain aspects of anatomic descriptions than actual anatomy studies, since it is done in vivo versus the traditional post-mortem approach.

This study established normal reference ranges for the thoracic and abdominal computed tomographic anatomy of clinically healthy common marmosets, including adapted CT protocols. This baseline study should facilitate CT examinations of marmosets in a clinical set-up and it is anticipated that diagnostic proficiency will be facilitated. The decision to perform advanced imaging is multi-factorial and highly dependent on patient factors, user experience with the modality and species, emotional value to the owner, availability and accessibility of equipment will be important decision criteria in developing decision strategies in clinical settings. Under ideal circumstances US is recommended as the screening tool of choice for the abdomen in the common marmoset. Radiography still plays an important role as a baseline imaging modality for the abdomen, particularly as whole body radiography in the common marmoset, providing simultaneous information about the thorax and the skeletal system; however its limitations must be considered. In cases where further work-up would be required or in certain clinical presentations, CT should be recommended and should always be combined with i.v. contrast.

TABLE OF CONTENTS

LIST OF FIGURES

LIST OF TABLES

GLOSSARY

ABBREVATIONS USED IN TEXT:

cm	centimeter
CT	computed tomography
Fig.	Figure
FOV	field of view
g	gram
GIT	gastrointestinal tract
HU	Hounsfield unit
i.v.	intravenous
kVp	kilovoltage peak
L	length
L1	1st lumbar vertebra (analogous for others)
mAs	milliampere-seconds
mg	milligram
MHz	megahertz
ml	milliliter
mm	millimeter
MRI	magnetic resonance imaging
n	number
OVAH	Onderstepoort Veterinary Academic Hospital
PSS	portosystemic shunts
ROI	region of interest
SD	standard deviation
US	ultrasonography
VD	ventrodorsal radiograph
W	width
WL	window level
WMdP	Wencke M. du Plessis
WW	window width

CHAPTER 1

1. GENERAL INTRODUCTION

The common marmoset is an arboreal small New World primate originating from South America, but has become a popular pet in certain parts of the world such as the Republic of South Africa. The common marmoset is frequently used as a small animal model in biomedical research, such as neuroscience[1,2] and to examine disease.[3,4]

Therefore, it must be clearly distinguished between wild and captive marmoset populations, as well as the common marmoset as pet or patient and lab animal kept as non-human small primate model for research purposes.

Some studies on marmosets were done in combination with imaging modalities such as radiography,[5, 6] computed tomography (CT)[7-9] including microcomputed tomography[10-12] and ultrasound (US).[13-17] Since the marmoset serves as a popular small animal model for neuroscience, there also exists extensive literature concerning very specialized magnetic resonance imaging (MRI), such as investigating whole-brain circuitry[18] and fetal sulcation and gyrification[19] to name just a few recent ones. It needs to be emphasized that the studies involving CT and MRI were done on marmosets as non-human small primate model for research purposes and most modalities therefore are either not readily available or not feasible for the private practitioner or not clinically applicable.

Common presenting diseases in the common marmoset include renal,[20-23] liver and skeletal disease.[22] But there are only sporadic case reports in the literature where diagnostic imaging has been used in the common marmoset as pet or patient, such as with calcinosis circumscripta[24] and metabolic bone disease.[25]

Diagnostic imaging has been used in other related species, such as the golden lion tamarin for radiographic evaluation of diaphragmatic defects.[26] Normal radiographic thoracic anatomy has been described in other non-human primates, such as the ring-tailed lemur[27] and vervet monkey.[28]

Ultrasound has been used in other non-human primates such as the cynomolgus monkey,[29-35] but also to describe the normal abdominal anatomy, such as in the vervet monkey.[36] It has been used as early as 1976 to evaluate the abdomen in rhesus monkeys.[37]

For the purpose of this dissertation the emphasis will be on the common marmoset as pet, and the study will be limited to such. This is based on the following: 1) As a pet the common marmoset is often presented to the Diagnostic Imaging Section, Onderstepoort Veterinary Academic Hospital (OVAH) and its associated Bird and Exotic Animal Hospital; 2) The lack of normal thoracic and abdominal CT anatomy prompted the main investigator to this study. 3) The emphasis based on above is on the feasibility to use CT for the private practitioner in the common marmoset as patient.

Similarly to above, the original lack of normal anatomy of any diagnostic imaging modality prompted the main investigator to previous descriptive ultrasonographic[38] and radiographic[39] anatomy in the common marmoset. Once

proper protocols and reference ranges were established, it enhanced the clinical potential of these modalities dramatically and was applied to clinical cases on a daily basis. A similar benefit is anticipated for the current study.

Therefore the current study was designed accordingly to answer the following main questions: What is “normal” for the common marmoset concerning CT of the thorax and abdomen? How does abdominal CT compare to other diagnostic imaging modalities such as radiography and ultrasonography and which modality should be recommended?

To the best of the principal investigator’s knowledge there has been no work published describing normal computed tomographic anatomy of the thorax and abdomen in the clinically normal common marmoset or associated species or a comparison done of different imaging modalities concerning its abdomen.

The study was approved by the University of Pretoria Ethics Committee.

1.1. Hypothesis

It is believed that dual CT can provide diagnostic quality images for the common marmoset despite its size and other limitations. Furthermore that normal thoracic and abdominal CT anatomy will assist in establishing what is normal for the common marmoset and point out significant species specific differences, which would form otherwise pitfalls for the private practitioner. However, it is hypothesized that standard CT protocols from small animals cannot just be transferred to exotic animals such as the common marmoset, but that

adaptations are needed. Furthermore that i.v. contrast will be at least beneficial, if not necessary, for abdominal CT studies. With increasing knowledge of CT thoracic and abdominal anatomy in clinically normal common marmosets it is anticipated that diagnostic proficiency will improve. However, the last point is beyond the scope of this study to prove and prompts further studies.

1.2. Objectives

i) Describe the CT thoracic anatomy in the clinically normal common marmoset

ii) Describe the CT abdominal anatomy in the clinically normal common marmoset

iii) Determine the normal reference range of Hounsfield units (HU) of major abdominal and thoracic organs

iv) Refine a protocol for abdominal and thoracic CT in the clinically normal common marmoset

v) Compare abdominal pre-and post-contrast CT findings

vi) Establish a CT abdominal atlas

vii) Compare different imaging modalities (particularly CT versus radiography, but also US) concerning the abdominal cavity in the common marmoset

1.3. Benefits of the study

Research was done by Wencke M. du Plessis and co-workers due to the need for a normal CT atlas including normal reference range in clinically normal common marmosets with the perspective to enhance the efficiency of this diagnostic imaging modality for future clinical applications.

i) Knowledge of the CT thoracic anatomy in the clinically normal common marmoset
ii) Knowledge of the CT abdominal anatomy in the clinically normal common marmoset
iii) Recommendations concerning CT protocols for the thorax and abdomen in the clinically normal common marmoset
iv) Recommendations concerning diagnostic imaging modalities concerning the abdomen of the common marmoset

CHAPTER 2

2. LITERATURE REVIEW

2.1. Marmosets

2.1.1. Classification

Marmosets (*Callithrix*), tamarins (*Saguinus* and *Leontopithecus*) and Goeldi's monkeys (*Callimico goeldii*) are small neotropical primates indigenous to South America. These three groups are classified as Callitrichidae.[22]

The common marmoset (*Callithrix jacchus*) is a small New World primate that is native to eastern Brazil. This species is listed as "Least Concern" by the International Union for Conversation and Nature.[40]

It has been used in biomedical research since the early 1960s.[41] Use of this species for research purposes continues to grow at a rapid pace as they are a viable alternative to other non-human primate species.[41] This is also emphasized by over 4400 articles that come up on a "PubMed" search when entering "marmoset" as a search item (as of December 2014), most of which are in the context of the common marmoset as an animal model for research.

The common marmoset in particular is a popular pet in South Africa and is commonly presented to the Exotic Animal Clinic of the OVAH.

2.1.2. Anatomy

It is interesting that based on its research model potential very detailed literature exist on the common marmoset,[18,19] including the entire genome sequencing.[42] However the most complete (macroscopic) anatomic description originates from 1927,[43] and there is no recent updated holistic literature available. A more recent general anatomy only exists in a similar species, such as the *Callimico goeldii*, but still originates from 1959.[44] Therefore terminology and taxonomy of Beattie[43] and other older literature is often either out-dated or used human terminology. For consistency purposes the older terminology was cited in quotation marks. Newer articles exist, however often only on selective anatomic areas or focusing on histology or morphometry.[45,46]

The literature review is divided into organ systems to facilitate incorporation of different literatures. Particularly concerning the skeletal system, there exists some controversy in the literature.

Skeletal system: The skeletal system will only be reviewed for parts relevant for the abdominal and thoracic imaging of this study, such as clavicle, sternum, ribs, thoracic vertebra, lumbar vertebra etc.

The number of cervical vertebrae is consistently reported to be 7,[39,47,48] however concerning the rest of the spine differences exist. Ankel-Simons[48] tabulates the number of vertebrae for the Callitrichidae as follows: 13/11 thoracic, 7/9 lumbar and 3 sacral vertebrae. The principal investigator found 7 cervical 12-13 thoracic, 6-7 lumbar and 3 sacral vertebrae in a previous study.[39] This is similar to another

study which reports of 12-13 thoracic, 6-7 lumbar and 2-3 sacral vertebrae. It also states that the thoracolumbar region always compromised of 19 vertebrae with 13 thoracic vertebrae predominantly.[47] Another study reports that the number of thoracic vertebrae varies even within the species (12 or 13),[43] and that the unstable character of the last thoracic vertebra (sometimes bearing a rib and sometimes becoming a lumbar vertebra) connects the “Hapalidae” with the higher primates.[43] The lumbar vertebrae number has been reported to be either six or seven depending on the number of thoracic vertebrae.[43]

The straight sacrum has been reported to consist of 3[39,43,48] or 2-3 sacral vertebrae,[47] which are fused[43] or at least in most cases fused.[47]

The most recent article on the skeletal system also describes the vertebrae in more detail:[47] The bodies of the thoracic vertebrae elongate towards the lumbar region resulting in a similar length of the thoracic and lumbar region despite the unequal vertebrae number.[47] The thoracic spinous process shortens and becomes broader towards the lumbar region.[47] The cranioventrally inclined transverse processes become larger towards the sacrum.[47] The last lumbar vertebra is the shortest lumbar vertebra.[47]

The anticlinal vertebra is reported to be the 9th thoracic vertebra (T9) or T10[47] as well as T9.[43]

The sternum consists of 7[43] or 6-7 segments depending on the number of thoracic vertebrae with a slender xiphoid process and broad manubrium with articular surfaces craniolaterally for the sigmoid clavicles connecting it with the

scapulae.[47] Subsequent sternebrae are connected to each other by means of intersternebral cartilages onto which the costal cartilages are attached.[47]

The number of ribs is dependent on the number of thoracic vertebrae and varies between 12 and 13.[43, 47] The 7th or 8th pair of ribs, depending on the number of thoracic vertebrae, is the last sternal pair that is directly attached to the sternum by costal cartilage.[47] The 8th costal cartilage is often fused to the 7th.[43] The 8th and 9th costal cartilages may fuse very close to the sternum, but do not reach it.[43] The 10th, 11th, 12th and 13th (if present) rib pairs are free.[43] Another author points out that the caudal pairs are asternal ribs that have indirect connections with the sternum since their costal cartilages are attached to that of the previous rib.[47] The last pair of ribs is very short and floating, thus lacking any connection with the sternum.[47]

Cardiovascular system: Beattie[43] is the only one reporting in detail on the cardiovascular system. The heart is four-chambered. He points out that there are 3 openings into the left auricle. The larger single opening is for the joined lobar pulmonary veins from the right lung, whereas the smaller two are from the separate lobar pulmonary veins from the "upper and lower" lobes of the left lung. The heart lies in the area of the 3rd to 6th articulation of the costal cartilage with the sternum. Compared to similar sized Tarsius and squirrel monkeys the heart appears smaller. Senos *et al.* state that the mean values for morphometry of the hearts did not show any significant difference between male and female common marmosets.[49]

Respiratory system: Two slightly newer articles focus not on the general anatomy, but on the morphology of the lungs[45] and the cytology of selected parts of the respiratory system.[46] The one study concludes that in comparison with mammals of similar size (rats, guinea pigs) it appears that the marmoset has a higher gas exchange capacity of the lung, which might reflect the athletic activity of this small primate.[45] An incidental finding worth mentioning is the individual variability of septal structures due to variations in capillary blood volume and hematocrit.[45]

The only macroscopic anatomical description concerning the respiratory system is once again from Beattie,[43] who reports that there are four lung lobes on the right and two on the left. The right lung consists of an “upper”, “ventral”, “lower” and “azygos” lung lobe. The “upper and ventral lobes” are folded over on themselves to produce a superficial and a deep lobule. The “lower” lobe is the largest and extends cranially to the 4th rib along the lateral thoracic wall and is in direct contact with the entire right cupola of the diaphragm. The “azygos” lobe is L-shaped. The left lung consists of two lobes – an “upper and a lower”, which are not subdivided by fissures. The greater part of the pericardium is separated from the diaphragm by the infra-cardiac recess of the right pleura for the “azygos” lobe of that lung.

Beattie also reports a gender dimorphism concerning the length of the trachea with females measuring 3 versus male about 4 cm.[43] There is a distinct gap between the dorsal ends of the rings.[43] The trachea divides into a right and left

main bronchus.[43] From the right main bronchus a branch arises which passes upwards into the “upper” lobe of the lung.[43] This is the “eparterial” bronchus.[43] Four main branches are given off to the right lung, that is one to each lobe.[43] On the left side the bronchus splits into two, an “upper and a lower” branch.[43]

Pleura: The right pleural cavity extends just a few mm cranially to 1st rib to the 1st lumbar vertebra.[43] The left pleural cavity does not extend as far caudally as the right.[43]

Digestive system: Initially the esophagus is dorsal to the trachea, then to the right from the thoracic inlet level to the bifurcation, then deviating to the left where it penetrates the diaphragm and runs in a fissure between the “left and caudate” lobe of the liver.[43] The crura of the diaphragm attach on the 1st-3rd lumbar vertebrae.[43]

The stomach consists of the relative large fundus, the body, the pyloric antrum and canal.[43] The body is separated from the pyloric antrum by a groove, which forms the *Incisura angularis* on the lesser curvature of the stomach.[43] The body tapers to the pyloric antrum to an even narrower short pyloric canal, which terminates at the pyloric sphincter.[43]

The stomach is situated in the abdomen under cover of the liver.[43] Only a small part of the anterior surface is in contact with the anterior abdominal wall.[43]

According to Ankel-Simons, many prosimian primates do not have a small intestine that can be subdivided into duodenum, jejunum, and ileum as in higher primates.[48]

The duodenum forms a J-shaped loop, with a long descending part on the right and a short transverse and ascending part.[43] The two latter parts hook round the lower border of the root of the mesentery.[43] The first part of the duodenum is very short.[43] The duodenum ends at a sharp flexure lying below the transverse meso-colon to which it is attached by a peritoneal band.[43] The anterior surface of the descending part of the duodenum is adherent to the upper layer of the transverse meso-colon.[43] The transverse colon is itself adherent to the duodenum where it crosses the descending loop.[43]

The remaining part of the small intestine (jejunum and ileum) form three short loops.[43] The ileum enters the colon ventromedially.[43]

The large intestine forms an inverted U-shaped loop and its length equals the crown-rump height of the animal.[43] The right limb consists of the caecum and the slightly shorter ascending colon.[43] The about 4 cm long caecum widens slightly towards its termination, which is hooked on itself, and lies in the caudal abdominal cavity without an *Appendix vermiformis*.[43]

Urinary system: Both kidneys lie at the same level at the 2nd to 3rd lumbar vertebrae.[43] They are kidney-shaped without lobulation with a relatively thick cortex.[43] The cranial aspect of the adrenal gland is flattened while the caudal

aspect is more pointed.[43] On the lateral wall of the small renal pelvis a single large pyramid is invaginated.[43]

The apex of the urinary bladder is prolonged into the “urachus” which stretches up on the inner surface of the abdominal wall.[43] The base of the bladder or trigone has three openings which lie close together – these are the openings of the ureters and the urethral opening.[43]

Glands associated with the digestive system (Liver and pancreas): The liver consists of four lobes (“central, left, right and caudate”).[43] The “central” lobe is divided into right and left halves by a fissure as well as the falciform ligament.[43] A deep fossa on the right half of the “central” lobe lodges the gall bladder which is not completely covered by liver tissue.[43] The “right” lobe is the largest one.[43] The “caudate” lobe has a deep fossa for the right adrenal gland and the cranial part of the right kidney.[43] No “accessory” lobes are present.[43] In prosimians the liver is usually much more divided than in higher primates.[48]

The pancreas consists of a vertical and transverse portion.[43] The transverse portion contacts the medial margin of the left adrenal gland and the left kidney.[43] The vertical part corresponds to the head, and the transverse part to the tail, of the human pancreas.[43]

Endocrine system (Adrenal glands): No detailed macroscopic anatomy description exists, despite numerous endocrinology or histochemical and histology articles.[50-52]

Lymphatic system: The spleen does not have a very well differentiated shape of its own, but rather changes easily on size, form and position of the adjoining organs such as the stomach.[48]

Reproductive system:

Male reproductive tract: The main literature is still from Beattie[43] and Hill.[44] The latter states that the testes are scrotal in position and are relatively large for the size of the animal – an unusual condition in the neotropical Primates.[44] The epididymis is almost half the size of the testis and the two are separated along their whole length by a digital fossa.[44]

Some slightly newer literature exists with the title "The male reproductive system of the common marmoset (*Callithrix jacchus*)",[53] however it focuses on the histology and histochemistry.

The prostate is located at the distal end of the urinary bladder and the glandular prostate does not completely surround the urethra.[54] The marmoset prostate is quite small and the two lobes are not visible on gross examination, but can be distinguished on histology.[54]

Female reproductive tract: The vagina is divided into a lower and upper part by a marked vaginal isthmus.[55] The mean length of the lower and upper vagina were 17 mm (34 mm in total vagina).[55] The mean uterine size was 8.4 (length) x 10.0 (width) x 6.4 (thickness) mm , with the ovary measuring 5.3 x 4.3 x 3.8 mm.[55] The vagina is proportionally long in comparison to the short uterine cavity.[55] Overall,

the anatomical relationship of the female reproductive tract is similar to humans.[55]

2.2. Computed tomography of the thorax

Compared with conventional radiography, computed tomography allows better distinction among specific tissue densities in the thorax and detection of subtle changes in organ size, shape, margin, contour, and position[56] and provides information about morphologic characteristics. Computed tomography is more sensitive to diagnose for example pleural effusion, pneumothorax, as well as more subtle pulmonary and bronchial disease than radiography.[57]

The CT thoracic anatomy has not only been described in cats,[58] dogs,[59,60] and goats,[61] but also more recently in some other more exotic species such as alpacas.[62]

However, to the best of the principal investigator's knowledge there has been no work published describing the computed tomographic thoracic anatomy in the clinically normal common marmoset.

2.3. Computed tomography of the abdomen

The CT abdominal anatomy has been described in cats[63] and dogs[64,65] and rabbits,[66] but also more recently in some other more exotic species such as alpacas and llamas.[67] More specialized organ system evaluations have been

described in dogs such as the CT characteristics of lymph nodes,[68] as well as the comparison of US and CT in sedated dogs.[69] And some clinical applications such as imaging findings (including CT) of ferrets diagnosed with lymphoma have been reported.[70]

To the best of the principal investigator's knowledge there has been no work published describing the computed tomographic abdominal anatomy in the clinically normal common marmoset.

CHAPTER 3

COMPUTED TOMOGRAPHIC THORACIC ANATOMY IN EIGHT CLINICALLY NORMAL COMMON MARMOSETS (*Callithrix jacchus*)

3.1. Introduction

The common marmoset (*Callithrix jacchus*) has become a popular pet in the Republic of South Africa and represents a common patient of the Diagnostic Imaging Section, Onderstepoort Veterinary Academic Hospital (OVAH) and its associated Bird and Exotic Animal Hospital. Common presenting diseases include renal, liver, and skeletal disease.[1,2] The lack of normal anatomy of any diagnostic imaging modality prompted the main investigator to describe the ultrasonographic[3] and radiographic[4] anatomy in the common marmoset as well as the abdominal anatomy via computed tomography (CT)[5] and a comparison to other diagnostic imaging modalities.[6]

Compared with conventional radiography, computed tomography allows better distinction among specific tissue densities in the thorax and detection of subtle changes in organ size, shape, margin, contour, and position[7] and provides information about morphologic characteristics. Computed tomography is more sensitive to diagnose for example pleural effusion, pneumothorax, as well as more subtle pulmonary and bronchial disease than radiography.[8]

The CT thoracic anatomy has not only been described in cats,[9] dogs[10, 11] and goats,[12] but also more recently in some other more exotic species such as and alpacas.[13]

However, to the best of our knowledge there has been no work published describing the normal computed tomographic thoracic anatomy in the common marmoset.

The purpose of this study was to describe the thoracic anatomy in clinically normal common marmosets by means of CT.

3.2. Materials and methods

Animals: Eight mature male (n=5) and non-pregnant female (n=3) marmosets (mean +/- standard deviation (SD) age, 23.6 +/- 14.5 months; range, 12 to 48 months) were included in this CT study. The animals were not related to each other. Clinical examination, complete blood count and liver, kidney, and pancreas specific biochemistry parameters were normal. They weighed 289.3 +/- 51.0 g; range, 235-365 g. The marmosets were fasted for 12 hours prior to scheduled procedures, but had free access to water. The marmosets were anaesthetised with Isoflurane inhalation (Isofor, Safe Line Pharmaceuticals, Florida, South Africa) to ensure safety of the handlers, to reduce motion artifacts during the CT examination and to minimise stress to the animals. This prospective study was approved by the University of Pretoria Ethics Committee.

***CT examination*:** A dual slice helical CT scanner (Siemens Emotion Duo, Siemens, Erlangen, Germany) was used. The marmoset was positioned in dorsal recumbency on a cushion with its head on a positioning device. Its arms and legs were taped in an extended position. A lateral digital survey image (scout) of the whole body of the marmoset was obtained. Transverse images of the whole body were acquired. A setting of 110 kVp and 35 mAs was used in combination with

an automatic exposure control. This included automatic tube current adaptation to the patient's size and anatomic shape together with an online controlled tube current modulation for each tube rotation (Care Dose 4D). It provided well-balanced image quality at low radiation dose level. All scans were acquired in a high frequency algorithm with edge enhancement ("inner ear" algorithm) with 1 mm collimation and craniocaudal scan direction. Matrix size was 512 x 512 with a pitch of 1.5. Scans were reconstructed in smooth kernels (H20s smooth) for mediastinal evaluation with the field of view (FOV) being targeted to the area of interest. However the minimum FOV was 50 mm. The images were viewed in the initial inner ear default settings (window level (WL) = 700 HU and window width (WW) = 4000 HU) as well as with soft tissue (WL = 40 HU and WW = 400 HU), lung (WL = -500 HU and WW = 1400 HU) and bone (WL = 300 HU and WW = 1500 HU) settings respectively.

Evaluation: The non-contrast CT images were evaluated by one examiner (WMdP) and findings recorded on a custom designed form using dedicated software (OsiriX open Source™ Version 3.9.1., OsiriX Foundation, Geneva, Switzerland).

In the bone window, thoracic relevant bony structures were evaluated and its numbers recorded, such as the thoracic vertebrae and sternebrae. The diameter of the thorax (height and width) was measured on transverse slices at the level of the 8th thoracic vertebra (T8). The angle of the trachea in relationship to the spine was subjectively described.

In the soft tissue window, on transverse images the height of the caudal vena cava and the aorta were recorded. In case of the esophagus it was recorded whether collapsed or dilated and whether gas filled.

In the lung window, on transverse images the diameter (height and width) including circumference of the trachea was measured at the thoracic inlet as well as 5-6 slices cranially to the bifurcation. On dorsal planes the angle between the main stem bronchi was recorded. The Hounsfield unit (HU) of the lung tissue was recorded bilaterally cranioventrally at T3 level, in the middle lung field at T8/T9 level as well as caudodorsally at T10 level. The round region of interest (ROI) was each time standardized to 0.1 cm^2, and was carefully placed to avoid major bronchi or blood vessels. Furthermore, the extend of the lung field was noted on dorsal images in relationship to both lungs, but also to bony landmarks, such as the ribs or thoracic vertebrae. On sagittal images the position of the carina was recorded in relationship to the thoracic vertebrae. Since this study was designed to be a descriptive study, data analysis was mainly limited to mean, standard deviations and range.

3.3. Results

Motion artifacts occurred commonly in close vicinity of the diaphragm, however all studies were considered to be of diagnostic quality. The inner ear algorithm subjectively provided good images, particularly considering the small size of the

common marmoset (Fig. 1). Tables 1 and 2 are the quantitative results of selected anatomic features.

Specific skeletal system features (Fig. 2)***:*** The clavicle was very prominent and attached to the also prominent triangular manubrium sterni, which was much wider than high. Only one animal had 12 thoracic vertebrae, whereas the remaining 7/8 animals had 13 thoracic vertebrae with 2/8 having some transitional features. The ribs of the last thoracic vertebrae were in both cases either uni- or bilaterally underdeveloped. However even when the vestigial ribs where of the same length than the adjacent transverse process of the following lumbar vertebra, it pointed caudally in contrast to the cranially pointing transverse processes of the lumbar vertebrae. The sternum consisted of the manubrium sterni, 4-5 sternebrae as well as the xiphoid process. The first rib pair attached at the cranial aspect of the manubrium sterni, the 2nd on the cranial aspect of each following sternebrae with multiple ribs attaching at the junction of the last sternebra and the xiphoid process followed by floating ribs.

Digestive system (Figs. 3 & 4)***:*** The esophagus was located to the left of the trachea and was either completely collapsed or partially gas filled. This occurred mainly in the thoracic inlet area and also just cranial to the diaphragm.

Cardiovascular system (Fig. 4)***:*** The heart, including the large blood vessels, could easily be distinguished. The cardiac apex pointed to the left of the sternum. The interventricular septum was not visible and individual blood vessels could not be distinguished within the cranial mediastinum. The pulmonary artery was

running laterally to the corresponding bronchus whereas the pulmonary vein was positioned medially, but often not directly adjacent to the corresponding bronchus. The pulmonary vein was usually ventral to the artery, however could be found at the same level of the pulmonary artery or even slightly dorsally to it (particularly on the right hemithorax). Subjectively the two vessels were of very similar size. The diameter of the caudal vena cava and aorta varied markedly, but had a similar maximal diameter.

Respiratory system (Figs. 3 & 4)***:*** The trachea followed the contour of the spine and ran parallel to it, only sloping slightly ventrally at the tracheal bifurcation. On transverse images, the trachea could be slightly flattened giving it a slightly inverted D sign at the level of the thoracic inlet area and was more rounded just cranial to the bifurcation. The carina was consistently located at the T5-T6 level. Cranially the lung extended to the 1st rib or 1st intercostal space. The bronchi were subjectively of similar size than the corresponding adjacent pulmonary artery and vein. Only the right middle bronchus had a dorsoventral orientation, and hence could be easily identified. Caudally the lung extended mostly to the middle of T12 (4/9), but could extend to the cranial aspect of T12 to midT13. There was no difference in the cranial and caudal extent between the right and left lung, even though the right side appeared often slightly more prominent. The accessory lung lobe could consistently be identified between the caudoventral mediastinum and the caudal vena cava (Fig. 4C).

Lymphatic system: None of the thoracic lymph nodes could be identified on non-contrast enhanced CT.

Pleura: Separation of the accessory lung lobe was consistently visible. Other separations of individual lung lobes were only inconsistently seen.

Mediastinum: the cranioventral mediastinum was prominent and v-shaped in a craniocaudal and dorsoventral direction, exceeding the width of the corresponding thoracic vertebrae. The caudoventral mediastinum was very thin.

3.4. Discussion

Exotic animals are being imaged more and more regularly via CT as well. However, due to their size and species specific anatomy, standard small animal CT protocols need to be critically assessed and adapted.

Considering the small size of the animal, the image quality was good. Motion artifacts did however occur and influenced the quality of some images. It occurred, particularly in the caudodorsal lung field, in close vicinity to the diaphragm. Due to the higher respiration rate of the marmoset in comparison to the dog, they will be more prone to this artifact. Should only thoracic CT images be desired a caudocranial scan direction should be chosen, further reducing motion artifacts. Hyperventilation, positive-pressure ventilation or another breath hold technique should also be considered. This was initially attempted in the first

two marmosets, however not successful and hence abandoned. However, despite motion artifacts and the small size of the marmosets, all thoracic images were considered to be of diagnostic quality. Use of newer generation multi-slice CT scanners would further minimize these motion artifacts due to reduced scan times and would be ideal, if available.

A high frequency algorithm with edge enhancement (“inner ear algorithm”) gave very good images, therefore it is recommended to acquire images in such an algorithm and also view them in those default settings (WL = 700 HU and WW = 4000 HU).

It should also be considered to position exotic species in dorsal recumbency for CT scans for a multitude of reasons, in contrast to the often recommended sternal recumbency in dogs. In this study, an i.v. catheter was placed in the femoral vein, which made comfortable and symmetric positioning in sternal recumbency not feasible. Additionally, dorsal recumbency enabled ready access to the catheter. Other benefits of the dorsal recumbency were believed to be less motion artifacts (both by respiratory and cardiovascular movement) since the patient is more stable positioned in dorsal recumbency and movement of the sternum during the respiratory cycle occurs. In contrast to larger animals such as dogs, smaller exotic species often have whole body diagnostic imaging performed.

Radiography certainly should remain the first diagnostic imaging modality for most thoracic imaging in the marmoset. However in selective cases, such as for assessment of thoracic metastasis, CT is considered the modality of choice.

Additionally for selective thoracic cases, such as more complex thoracic pathology, further diagnostic imaging work-up including CT should be considered. Another advantage of CT is the possibility of CT-guided biopsies. The tomographic character of CT also overcomes the limitations of superimposition encountered by radiography, which particularly affects radiography of the cranial thoracic cavity in the marmoset. Computed tomography also has better soft tissue differentiation capabilities; hence enabling clear assessment of the cranial aspect of the cardiac silhouette, which is often hampered radiographically.

It must be remembered that for complete evaluation the thoracic cavity should be analysed in a lung, soft tissue and bone algorithm. Positional CT should also be considered depending on the area of interest, because of gravity dependent atelectasis and pleural fluid accumulation.

Comparison of mean densitometric CT values obtained during helical CT scans reconstructed in a sharp algorithm was -846 HU in dogs[14] and -712.1 HU of the caudal right lung and -726.8 of the caudal left lung of the clinically normal Saanen goats.[12] The HUs obtained in this study differed from those (Table 2), and emphasized the importance of establishing normal ranges for different species, since the microanatomy differs in species. Furthermore, this study also demonstrated that lung HUs differed even in the same animal depending on where it was obtained. The value of the HUs differed in the cranioventral, middle and caudodorsal lung field with the accessory lung lobe having the highest values followed by the caudodorsal lung field. This is believed to be due to

gravity dependent atelectasis. Therefore location of measurement, positioning, duration of positioning, anesthesia protocol and the respiration cycle have to be taken into consideration when assessing the HU of the different lung areas. Should atelectasis be suspected positional CT should be considered. The ROI of 0.1 cm^2 was chosen as large as possible to include the largest possible parenchymatous area without including non-parenchymatous tissues (large pulmonary blood vessels and larger bronchi) consistently. A larger ROI would have included the above, hence affecting the mean HU values. In contrast to smaller ROIs might not cover a large enough area, potentially limiting the ability to resolve small lesions[15] or may not be representative of the tissue. Since CT evaluation via HU unit is an indirect method of assessing the lung tissue, disease processes that result in replacement of air-filled structures result in higher HU. And disease processes that result in an increased amount of airspace such as with emphysema or other air-trapping diseases result in reduced HU.

It should be considered that CT might be better for certain aspects of anatomic descriptions in live animals than in cadaveric anatomy studies.[16] The main author believes that this is even more essential for descriptive studies of dynamic organ systems such as the respiratory and cardiovascular system.

3.5. Conclusion

This study provided a detailed anatomic description of the thorax in clinically healthy marmosets by means of CT. It emphasized that diagnostic quality images

can be obtained of the marmoset despite its small size and high respiratory rate using a dual slice CT scanner. Therefore, CT examination of marmosets in a clinical set-up is feasible and having normal references will assist the veterinarian using CT for thoracic evaluation in this species.

3.6. References

1. Montali RJ, Bush M. Diseases of the Callitrichidae. In: Fowler M (ed): *Zoo and Wildlife Medicine, 4th ed*. Philadelphia: WB Saunders Company, 1999;369-376.

2. Ludlage E, Mansfield K. Clinical care and diseases of the common marmoset (*Callithrix jacchus*). *Comparative Medicine*. 2003;**53**: 369-382.

3. Wagner WM, Kirberger RM. Transcutaneous ultrasonography of the abdomen in the normal common marmoset (*Callithrix jacchus*). *Veterinary Radiology & Ultrasound*. 2005;**46**: 251-258.

4. Wagner WM, Kirberger RM. Radiographic anatomy of the thorax and abdomen of the common marmoset (*Callithrix jacchus*). *Veterinary Radiology & Ultrasound*. 2005;**46**: 217-224.

5. du Plessis WM, Groenewald HB, Elliot D. Computed tomography of the abdomen in eight clinically normal common marmosets (*Callithrix jacchus*). 2015, submitted for publication.

6. du Plessis WM, Groenewald HB. Abdominal computed tomographic atlas in clinically normal common marmosets (Callithrix jacchus) and comparison of

computed tomography to other imaging modalities. *2015*, submitted for publication.

7. Stickle RL, Hathcock JT. Interpretation of computed tomographic images. *The Veterinary Clinics of North America Small Animal Practice*. 1993;**23**: 417-435.

8. Prather AB, Berry CR, Thrall DE. Use of radiography in combination with computed tomography for the assessment of noncardiac thoracic disease in the dog and cat. *Veterinary Radiology & Ultrasound.* 2005;**46**: 114-121.

9. Henninger W. Use of computed tomography in the diseased feline thorax. *The Journal of Small Animal Practice*. 2003;**44**: 56-64.

10. De Rycke LM, Gielen IM, Simoens PJ, van Bree H. Computed tomography and cross-sectional anatomy of the thorax in clinically normal dogs. *American Journal of Veterinary Research*. 2005;**66**: 512-524.

11. Rivero MA, Ramirez JA, Vazquez JM, Gil F, Ramirez G, Arencibia A. Normal anatomical imaging of the thorax in three dogs: computed tomography and macroscopic cross sections with vascular injection. *Anatomia, Histologia, Embryologia*. 2005;**34**: 215-219.

12. Ohlerth S, Becker-Birck M, Augsburger H, Jud R, Makara M, Braun U. Computed tomography measurements of thoracic structures in 26 clinically normal goats. *Research in Veterinary Science*. 2012;**92**: 7-12.

13. Cooley SD, Schlipf JW, Jr., Stieger-Vanegas SM. Computed tomographic characterization of the pulmonary system in clinically normal alpacas. *American Journal of Veterinary Research*. 2013;**74**: 572-578.

14. Morandi F, Mattoon JS, Lakritz J, Turk JR, Wisner ER. Correlation of helical and incremental high-resolution thin-section computed tomographic imaging with histomorphometric quantitative evaluation of lungs in dogs. *American Journal of Veterinary Research*. 2003;**64**: 935-944.

15. Mayo JR. High resolution computed tomography. Technical aspects. *Radiologic Clinics of North America*. 1991;**29**: 1043-1049.

16. Beattie J. The Anatomy of the Common Marmoset (*Hapale jacchus Kuhl*). *Proceedings of the Zoological Society in London*, 1927;593-718.

3.7. Tables

Table 1. Measurements of the thorax of the common marmoset using CT

Variable	Mean	Standard deviation	Range	
			Minimum	Maximum
Thoracic diameter at T8 [mm]				
Height	2.48	0.28	2.05	2.80
Width	3.09	0.32	2.66	3.48
Caudal vena cava diameter [mm]	0.30	0.07	0.21	0.41
Aorta diameter [mm]	0.26	0.07	0.18	0.39
Trachea diameter at thoracic inlet				
Height [mm]	0.33	0.06	0.25	0.44
Width [mm]	0.29	0.06	0.23	0.40
Circumference [cm2]	0.08	0.03	0.05	0.14
Trachea diameter just cranial to carina				
Height [mm]	0.27	0.02	0.23	0.31
Width [mm]	0.27	0.03	0.23	0.33
Circumference [cm2]	0.06	0.02	0.04	0.10
Angle of mainstem bronchi [°]	56.47	7.33	40.73	64.87

Table 2. Hounsfield units of the lungs of the common marmoset

Measurement location	Mean	Standard deviation	Range	
			Minimum	Maximum
Cranioventral lung field at T3 level				
Right	-748.89	31.86	-800.97	-702.78
Left	-806.16	43.36	-868.25	-746.49
Middle lung field at T8 level				
Right	-699.82	58.91	-777.80	-620.73
Left	-696.06	95.51	-883.19	-574.52
Accessory	-548.64	87.23	-675.18	-427.90
Caudodorsal lung field at T10 level				
Right	-660.38	73.17	-768.64	-521.84
Left	-649.30	70.33	-737.59	-500.35

3.8. Figures

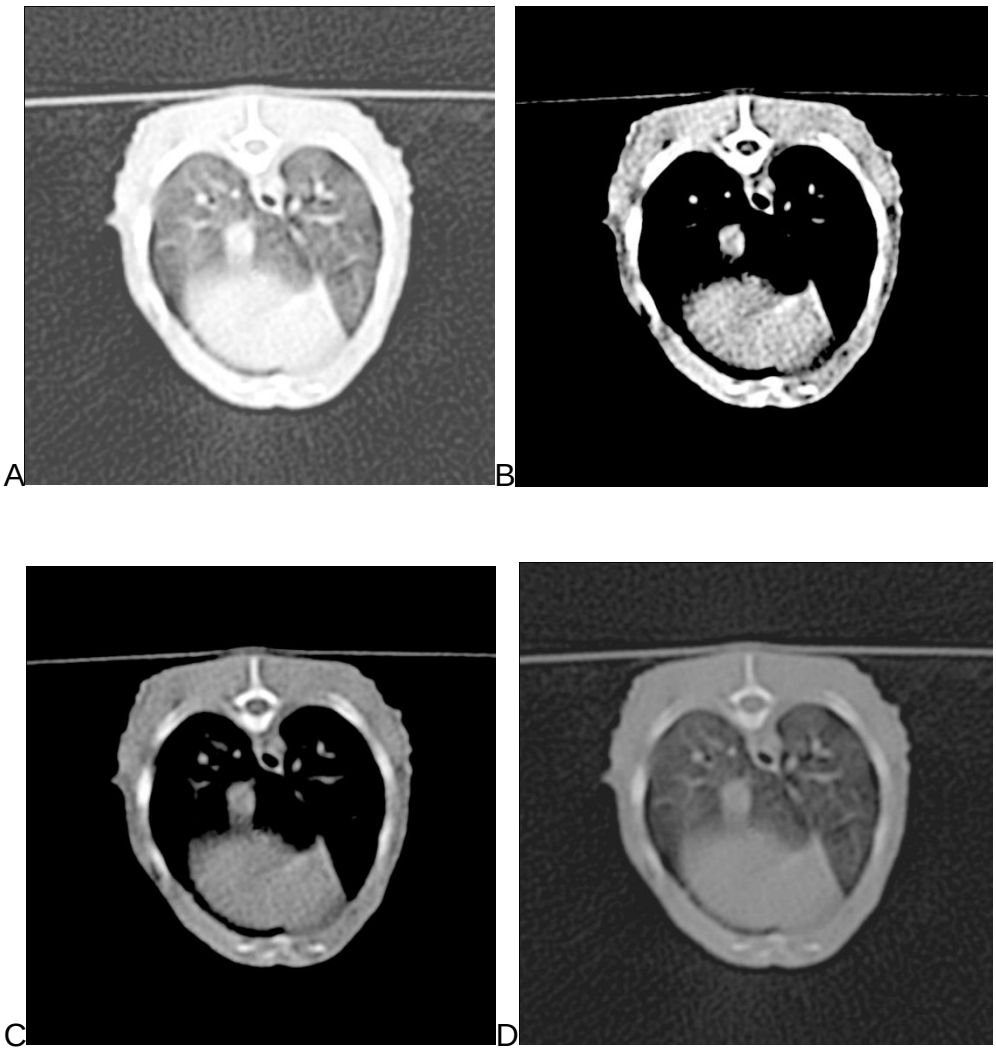

Fig. 1: Transverse CT images of a 16-month-old male common marmoset viewed with different windows. Dorsal is on the top and right on the left of the images. (A) Lung window (WL = -500 HU and WW = 1400 HU), (B) soft tissue window (WL = 40 HU and WW = 400 HU), (C) bone window (WL 300 HU and WW = 1500 HU) and (D) default settings of the inner ear algorithm (WL = 700 HU and WW = 4000 HU). The latter gave the best overall visibility of all relevant anatomic structures. For anatomic annotation please consult Fig. 4C.

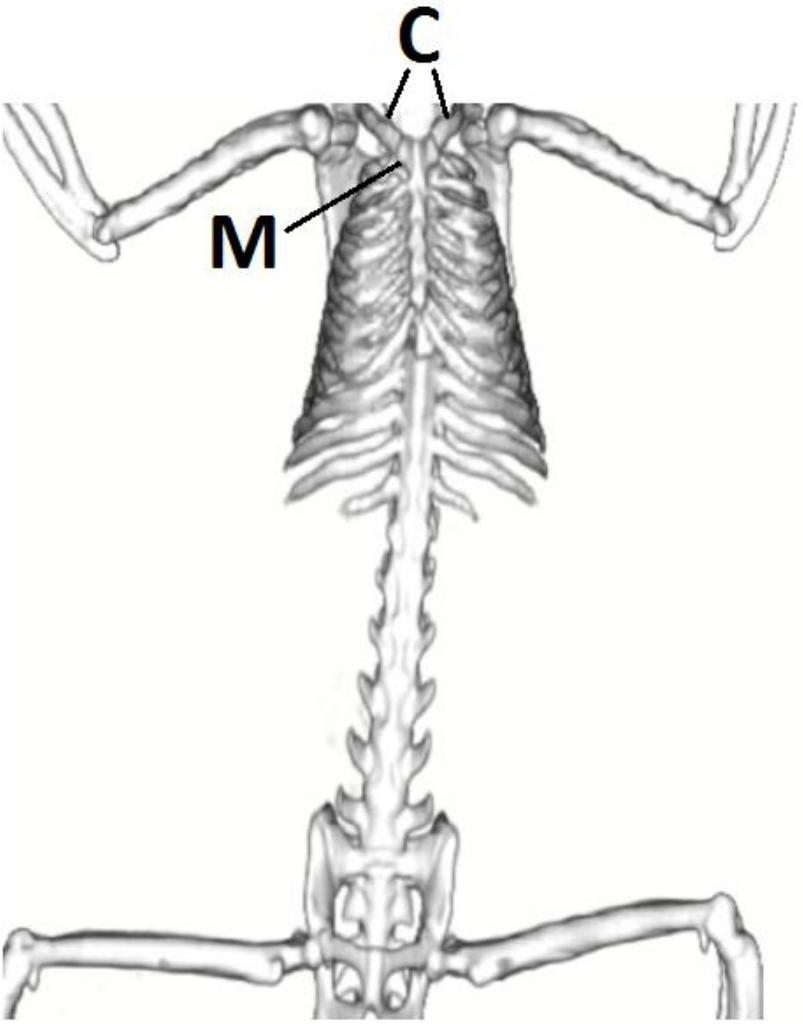

Fig. 2: Ventral view of a 3D-Volume CT reconstruction of the skeleton of a 21-month old female common marmoset. Take note of the prominent clavicles (C) and manubrium sterni (M). This marmoset had 13 thoracic vertebra, 6 lumbar vertebrae and 3 sacral vertebrae. The last thoracic vertebra often had transitional characteristics, but even when a rib was not prominently developed it angled always caudally, in contrast to the transverse processes of the lumbar vertebra that angled always cranially.

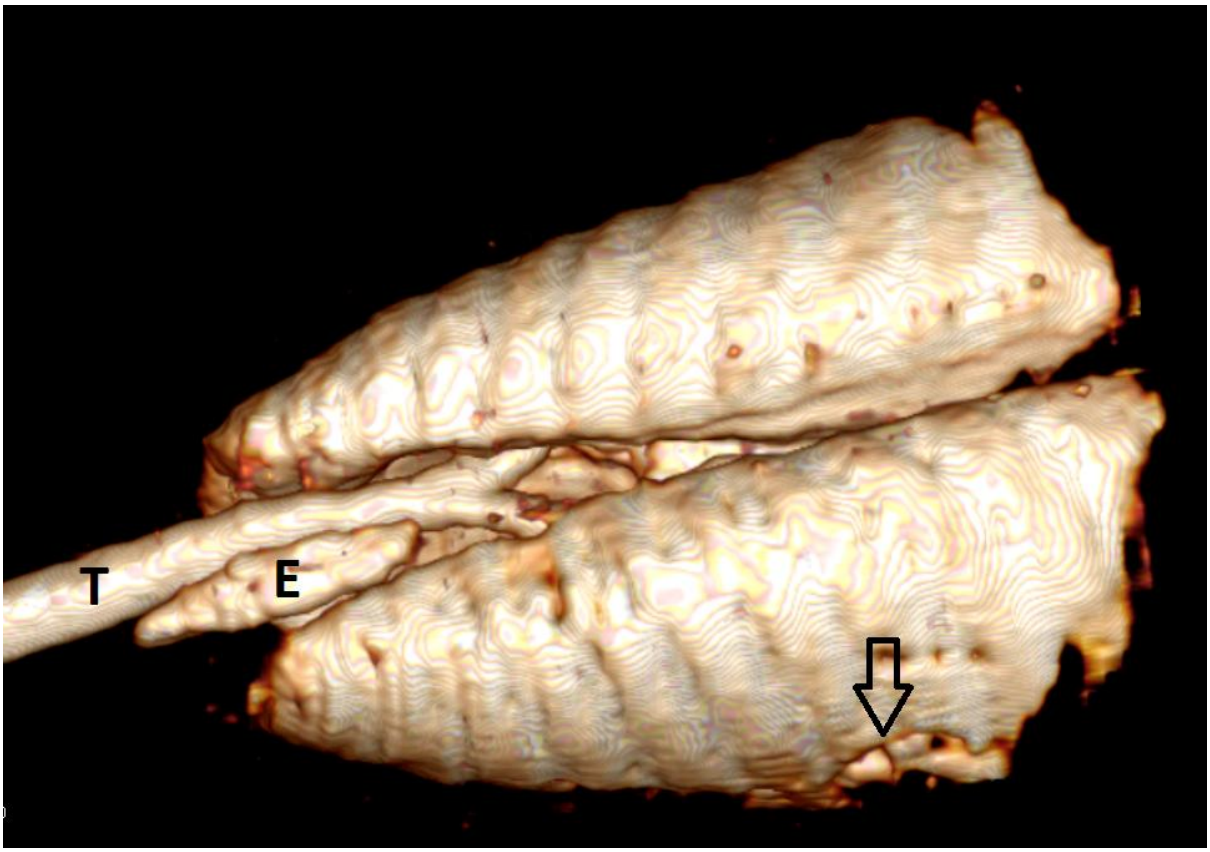

Fig. 3: Dorsal view of 3D CT lung reconstruction of a 21-month-old female common marmoset. Note the gas filled esophagus (E) to the left of the trachea (T), the mainstem bifurcation as well as the indentation of the ribs and the cardiac incisura (arrow).

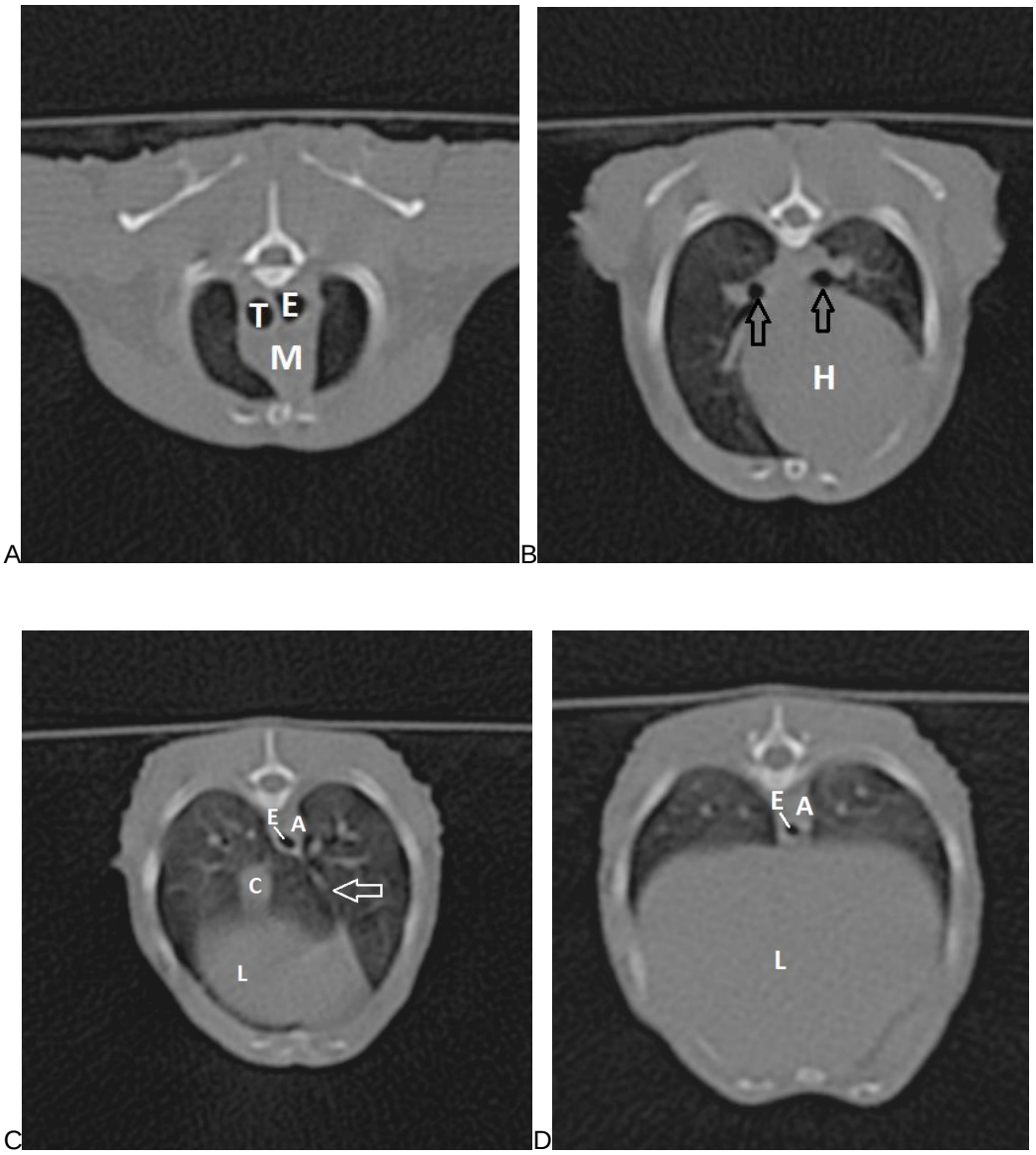

A B C D

Fig. 4: Representative transverse images of the thorax using the default settings of the inner ear algorithm (WL = 700 HU, WW = 4000 HU). Dorsal is on top and right on the left of the images. (A) The cranial mediastinum (M) is wider than the width of the corresponding thoracic vertebra. The esophagus (E) is gas filled and to the left of the trachea (T). (B) The apex of the heart (H) is on the left to the sternum, hence resulting in the left lung being less prominent than the right at this level. The bronchi are indicated by arrows. (C) Same image as Fig. 1D, but

annotated. The accessory lung lobe could consistently be identified between the caudoventral mediastinum (white arrow) and the caudal vena cava (C). The aorta (A) is dorsal and to the left of the gas filled esophagus. (D) The caudal lungfield is dominated by the prominent liver (L).

CHAPTER 4

COMPUTED TOMOGRAPHY OF THE ABDOMEN IN EIGHT CLINICALLY NORMAL COMMON MARMOSETS (*Callithrix jacchus*)

4.1. Introduction

Diagnostic imaging is more and more commonly used for clinical work-up of exotic animals. The common marmoset (*Callithrix jacchus*) is often presented at the Diagnostic Imaging Section, Onderstepoort Veterinary Academic Hospital (OVAH) and its associated Bird and Exotic Animal Hospital. Common presenting diseases include renal, liver, and skeletal disease.[1,2] In the common marmoset normal abdominal ultrasonographic[3] and radiographic[4] anatomy as well as the thoracic anatomy via computed tomography (CT)[5] and a comparison of abdominal CT to other imaging modalities[6] has been described. A high frequency algorithm with edge enhancement proved to be beneficial for the evaluation of thoracic CT[5] in clinically normal common marmosets.

The CT abdominal anatomy has been described in cats[7] and dogs[8,9] and rabbits,[10] but also more recently in some other more exotic species such as alpacas and llamas.[11] More specialized organ system evaluations have been described in dogs such as the CT characteristics of lymph nodes,[12] as well as the comparison of ultrasound and CT in sedated dogs.[13] And some clinical applications such as imaging findings (including CT) of ferrets diagnosed with lymphoma have been reported.[14]

To the best of the authors' knowledge there has been no work published describing abdominal CT in the common marmoset.

The aim of this study was to provide a detailed anatomical description of the abdomen in the clinically normal common marmoset by means of CT.

Furthermore to determine the normal reference range of Hounsfield units (HU) of major abdominal organs and to determine good settings for a CT protocol for the common marmoset.

4.2. Materials and methods

Animals: Eight unrelated mature male (n=5) and non-pregnant female (n=3) marmosets (mean +/- SD age, 23.6 +/- 14.5 months; range, 12 to 48 months) were included in this CT study. They were clinically healthy based on physical examination and routine haematological and biochemical analysis. They weighed 289.3 +/- 51.0 g; range, 235-365 g. The marmosets were fasted for 12 hours prior to scheduled procedures, but had free access to water. The marmosets were anaesthetised with Isoflurane inhalation (Isofor, Safe Line Pharmaceuticals, Florida, South Africa) to ensure safety of the handlers, to reduce motion artifacts during the CT examination and to minimise stress to the animals. This prospective study was approved by the University of Pretoria Ethics Committee.

CT examination: A dual slice helical CT scanner (Siemens Emotion Duo, Siemens, Erlangen, Germany) was used. The marmoset was positioned in dorsal recumbency on a cushion with its head on a positioning device. Its arms and legs were taped in an extended position. A lateral digital survey image (scout) of the whole body of the marmoset was obtained. Transverse images of the whole body were acquired from cranial to the diaphragm to caudal to the pelvis. A setting of

110 kVp and 35 mAs was used in combination with an automatic exposure control. This included automatic tube current adaptation to the patient's size and anatomic shape together with an online controlled tube current modulation for each tube rotation (Care Dose 4D). It provided well balanced image quality at low radiation dose level. All scans were acquired in a high frequency algorithm with edge enhancement ("inner ear" algorithm) with 1 mm collimation and craniocaudal scan direction. Matrix size was 512 x 512 with a pitch of 1.5.

For the post-contrast study, 1 ml/kg of Omnipaque 350 mg I/ml (Amersham Health (Pty) Ltd, Constantia Park, South Africa) with a 0.05 ml chaser was injected manually into the femoral vein via i.v. catheter with image acquisition directly afterwards (venous phase).

The images were viewed in the inner ear default settings (window level (WL) = 700 HU and window width (WW) = 4000 HU) as well as with soft tissue (WL = 40 HU and WW = 300 HU) settings and bone (WL = 300 HU and WW = 1500 HU) settings respectively. Additionally images were evaluated using WL = 50 HU and WW = 600 HU. The cranial abdomen was also assessed using a mediastinal setting of WL = 40 HU and WW = 400 HU. Pertaining to the urinary system, WL = 100-200 HU and WW = 300-400 HU as well as WL = 300-500 HU and WW = 1000-1600 HU were assessed focussing on WL = 500 HU and WW = 1600 HU.

Evaluation: The CT images were evaluated by one examiner (WMdP) and findings recorded on a custom designed form using dedicated software (OsiriX open Source™ Version 3.9.1., Osirix Foundation, Geneva, Switzerland).

Abdominal organs were identified and visibility noted on pre- and post-contrast images. Individual settings were compared with each other. The ROI was standardized for each individual organ ranging from 0.02 cm^2 for small organs such as adrenals and ovaries to 0.1 cm^2 for large organs such as the liver.

Since this study was designed to be a descriptive study, data analysis was limited to mean, standard deviations and range.

4.3. Results

The i.v. catheter could not be successfully placed in the first common marmoset, therefore only 7 post-contrast studies were performed.

The inner ear algorithm provided subjectively reasonable images (Fig. 1). Using its default settings, contrast could not be appreciated on post-contrast images. When manipulated to WL = 50 HU and WW = 600 HU contrast in the post-contrast images became visible and the overall abdominal detail was good. When using the same window (WL = 50 and WW = 600 HU) for abdominal settings (Fig. 2), contrast was not as clearly visible as on the original images, but still overall good. Viewing the post-contrast images with WL 500 HU and WW = 1600 HU did not provide additional information, and were not considered of superior quality but rather too dark and did not distinguish contrast-uptake from non-enhancing tissue. Same applied for viewing the urinary system using WL = 100-200 HU and WW = 300-400 HU as well as WL = 300-500 HU and WW =

1000-1600 HU. Viewing the cranial abdomen with mediastinal settings did not provide any additional information.

The most commonly encountered artifacts were the motion artifacts in close vicinity of the diaphragm as well as high-density streak artifacts from the metal component of the catheter in the hind limb as well as high-density streak artifacts and blooming from the positive contrast medium, particularly in the liver.

For detailed pre- and post-contrast HU of individual organs please consult Tables 1 & 2.

Relevant skeletal system: All animals consistently had 6 lumbar vertebrae. The ribs of the last thoracic vertebra were either uni- or bilaterally underdeveloped in 2/8 animals giving it some transitional features. However even when the underdeveloped ribs were of the same length than the adjacent transverse process of the following lumbar vertebra, they pointed caudally contrary to the cranially pointing transverse processes. The sacrum consisted of 3 segments.

Vascular system: The caudal vena cava was much more prominent than the abdominal aorta at the same level (often up to about 2-3 times). On transverse images, the renal veins were each time prominently visible. Post-contrast 3D CT reconstruction facilitated identification of individual blood vessels.

Lymphatic system: The spleen could be identified in the left abdomen, dorsally and cranially to the left kidney. It was fairly isodense to the kidneys, but hypodense to the liver on pre-contrast, and hypodense to kidneys and liver on post-contrast images.

Peritoneum: It contained varying degrees of fat. Larger amounts of intraabdominal fat enhanced the visibility of abdominal organs and enabled easier detection.

Reproductive tract: Ovaries could be seen as well as the uterus. The testes were easily visible if included in the scan area (2/5).

Gastrointestinal tract: The terminal part of the oesophagus in the thoracic cavity often contained varying degrees of focal gas accumulations. The oesophagus could not be seen intra-abdominal, but entered the diaphragm in a central position. The stomach was mainly positioned in the left abdomen, without direct contact with the diaphragm. The pylorus was fairly centrally positioned and only extended slightly to the right of the midline. No gastric folds were visible. The stomach often contained fluid, which on post-contrast images could be clearly distinguished from the enhanced wall. The duodenum could only occasionally be seen exiting the stomach. The small intestine was short and contained only a small amount of gas, contrary to the large intestine. The cecum contained a mottled gas-ingesta mixture giving it an almost honeycomb-appearance and

could consistently be identified. It was prominent and the base was in the craniodorsal abdomen, coursing caudoventrally along the right abdominal wall with fairly homogeneous diameter. The apex remained prominent and only narrowed to about half its diameter. It coursed cranially and medially. The remaining part of the large intestine presented as an inverted U with short ascending, transverse and descending colon. The descending colon was laterally and slightly ventrally to the left kidney. The ascending colon was ventromedially to the right kidney. The large intestine contained fecal balls or gas. The walls of the gastrointestinal tract enhanced markedly on post-contrast.

Urinary tract: The right kidney was in direct contact with the liver, which hampered clear outline of its cranial margin. Both kidneys were of similar size, oval-shaped and positioned between L1-L3. The right kidney was positioned cranially to the left kidney in 3/8 animals (Fig. 3) and caudally in 5/8 animals. Sometimes fat could be seen as eccentric hypodensity. The bladder was often empty and cranial to the pelvic inlet. Ureters could be seen using the modified inner ear setting at WL = 50 HU and WW = 600 HU, and not very clearly on the abdominal one (Fig. 4). They were more easily visible on post-contrast studies (Fig. 5) and started fairly centrally ventral to the spine and coursing laterally further caudally.

Adrenals: The adrenals were prominent in the common marmoset. The right adrenal was more difficult to appreciate on pre-contrast images due to its close

proximity to other soft tissue density tissues such as the liver and right kidney. The left adrenal was easily detectable; however contrast facilitated easier detection of both and cranial demarcation of the right. No corticomedullary distinction was visible on any images. The adrenals were fairly isodense on pre-contrast images, and took contrast up strongly immediately, however to a lesser degree than the kidneys (hypodense to kidneys).

Liver and gallbladder: The right side of the liver was markedly more prominent than the left (Fig. 3). No individual fissures between liver lobes could be identified. On post-contrast images, the liver parenchyma enhanced markedly accentuating hepatic vasculature. The gallbladder wall did not take up contrast. Since the lumen of the gallbladder did not take up contrast, it became easier visible on post-contrast images as relative hypodense structure in relationship to the hyperdense liver parenchyma. The gall bladder was surrounded by liver tissue and positioned on the right. The liver was hyperdense compared to the kidneys on pre-contrast images, but became fairly isodense on post-contrast images.

The pancreas and prostate could not be identified. Abdominal lymph nodes could only occasionally and inconsistently be seen after contrast-medium application.

4.4. Discussion

Exotic animals are being imaged more and more regularly via CT. However due

to their size and different anatomy, standard small animal CT protocols need to be critically assessed and adapted.

All studies were considered to be of diagnostic quality, and abdominal detail was enhanced by abdominal fat. Due to the small size and the limited resolution of dual slice CT scanners, interpretation of pre-contrast abdominal CT images of the common marmoset were challenging and limited, and i.v. contrast improved the adequate identification and interpretation of the abdomen significantly. Therefore i.v. contrast should be part of a complete standard abdominal CT evaluation of the common marmoset. Depending on the clinical indication, other contrast procedures of the gastrointestinal (barium or iodine), urogenital and lymphatic system should be considered. Additionally, delayed vascular studies might provide additional information of the biliary system, since iodine based contrast media are excreted in small fractions into the biliary system. Hence approximately 30-60 min post contrast hepatic and biliary system (including gall bladder) accumulation has been reported in small animals.[15] However, none of these studies have been described in the common marmoset.

Post-contrast 3D CT reconstructions were considered particularly helpful for vascular evaluation, but also the gastrointestinal tract (GIT). The 3D CT reconstructions also assisted with anatomic identification and for a better topographic understanding. For example, even though both kidneys were reported to be at L1-L3, they were either both at the same level (4/8) or the right kidney was cranial to the left kidney (4/8). This is contrary to an anatomic study were both kidneys are described at L2-3 and at similar level.[16] This might be due

to the fact that the study population really differed or alternatively could indicate that CT (particularly when using 3D reconstructions) renders better anatomical information than the actual traditional post-mortem dissections. Furthermore, the difference in position of the kidneys noticed in this study (same level or right kidney cranial to left kidney) might also imply that the kidneys in the marmoset are quite moveable similar to cats. It is believed that CT might be better for certain aspects of anatomic descriptions than actual anatomy studies,[16] since it is done in vivo versus the traditional post-mortem approach. This is believed to be even more essential for dynamic organ systems such as the digestive and the vascular system.

Dorsal recumbency was used contrary to the often used sternal recumbency in small animals, since an i.v. catheter was placed in the hind leg and the common marmoset could be better positioned in dorsal recumbency. No obvious disadvantage was noted. On the contrary, it was felt that it gave the abdominal content more room to spread resulting in less compression of abdominal organs. Independently, positional CT should be considered in individual cases, using gravity to shift both freely movable fluid and gas to give additional information.

Considering the size of the patient, the image quality was good. Motion artifacts did however occur and influenced the quality of some images. Using a cranial to caudal scan orientation as described in this study will however minimize this artifact. The use of newer generation multi-slice CT scanners would further minimize these motion artifacts; however they are not yet readily available in general private practice.

Initially the Inner ear algorithm was not believed to be as beneficial as in the thoracic cavity[5] for multiple reasons, but particularly since the post-contrast images didn't show up contrast at all. However after window manipulation, it proved to be beneficial and rendered additional information. The inherent edge enhancement of this algorithm enabled the visibility particularly of smaller structures such as the ureters and gave more detailed information concerning finer structures.

For complete evaluation the abdominal cavity in small animals should be viewed with soft tissue and bone settings; One article described additional viewing of the cranial abdomen in dogs with a mediastinal window,[9] which was not found to be beneficial in the common marmoset.

Based on the findings in this study, the following protocol should be used for the common marmoset: Inner Ear default settings of WL = 700 HU and WW = 4000 HU modified to WL = 50 HU and WW = 600 HU for both pre-and post-contrast images. On a soft tissue window it should be viewed at WL = 40 HU and WW = 300 HU, with post-contrast images set on WL = 50 HU and WW = 600 HU. Concerning small animals the benefit of viewing CT images concerning the urinary system with WL = 100-200 HU and WW = 300-500 HU and post-contrast images with WL = 300-500 HU and WW = 1000-1600 HU has been described.[17] However when viewing images with those settings no improvement concerning evaluation of the urinary system was noted. Using settings of WL = 500 HU and WW = 1600 HU contrast could not delineate non-enhancing structures and the images were too dark. The bone window (WL = 300 HU and

WW = 1500 HU) could also be considered, however the original default inner ear setting already provided adequate information.

The size of the ROI varied between different organs since it was selected as large as possible to represent the investigated tissue adequately without falsely influencing it by larger structures. Assessing abdominal tissue via CT by means of HU is only an indirect method. The HU of the liver has been reported as 42-65 HU in the cat and 60-70 in the dog[15] contrary to 108.04 +/- 13.6 (left) and 104.77 +/- 7.4 (right) liver in the common marmoset. The HU of the adrenals were also higher with 57.44 +/- 12.56 left adrenal and 56.57 +/- 9.48 right adrenal versus 36.0 +/- 5.3 and 34.3 +/- 7.0.[18] The post-contrast values of the adrenals were very similar (around 100 HU).[18] The difference in HU of individual organs compared to the common marmoset, emphasized again the importance of establishing individual normal ranges for different species and knowing species specific anatomic differences.

The proposed protocol of this study should be seen as a recommendation, since it must be taken into consideration that ideal window settings are subjective, and hence may need to be adjusted. It is also important to note that the average HU of the abdominal organs of the common marmoset proved to be higher than that in small animals. Therefore, depending on the area of interest, it should even be considered to adjust the window level even further to 75-100 depending on the organ of interest with a low window width (500-600) to enhance contrast.

4.5. Conclusion

This study provides information on abdominal CT in clinically healthy marmosets. Diagnostic quality images could be obtained of the abdomen of the common marmoset despite its small size using a dual slice CT scanner. Therefore, CT should be considered as a complimentary diagnostic imaging modality in cases requiring further work-up in the common marmoset and should always be combined with i.v. contrast administration. However due to their size and different anatomy, standard small animal CT protocols need to be critically assessed and adapted.

4.6. References

1. Montali RJ, Bush M. Diseases of the Callitrichidae. In: Fowler M (ed): *Zoo and Wildlife Medicine, 4th ed*. Philadelphia: WB Saunders Company, 1999;369-376.

2. Ludlage E, Mansfield K. Clinical care and diseases of the common marmoset (*Callithrix jacchus*). *Comparative Medicine*. 2003;**53**: 369-382.

3. Wagner WM, Kirberger RM. Transcutaneous ultrasonography of the abdomen in the normal common marmoset (*Callithrix jacchus*). *Veterinary Radiology & Ultrasound*. 2005;**46**: 251-258.

4. Wagner WM, Kirberger RM. Radiographic anatomy of the thorax and abdomen of the common marmoset (*Callithrix jacchus*). *Veterinary Radiology & Ultrasound*. 2005;**46**: 217-224.

5. du Plessis WM, Groenewald HB, Elliot D. Computed tomographic thoracic anatomy in eight clinically normal common marmosets (*Callithrix jacchus*). 2015, submitted for publication.

6. du Plessis WM, Groenewald HB. Abdominal computed tomographic atlas in clinically normal common marmosets (*Callithrix jacchus*) and comparison of computed tomography to other imaging modalities. 2015, submitted for publication.

7. Samii VF, Biller DS, Koblik PD. Normal cross-sectional anatomy of the feline thorax and abdomen: comparison of computed tomography and cadaver anatomy. *Veterinary Radiology & Ultrasound.* 1998;**39**: 504-511.

8. Teixeira M, Gil F, Vazquez JM, Cardoso L, Arencibia A, Ramirez-Zarzosa G, et al. Helical computed tomographic anatomy of the canine abdomen. *Veterinary Journal*. 2007;**174**: 133-138.

9. Rivero MA, Vazquez JM, Gil F, Ramirez JA, Vilar JM, De Miguel A, et al. CT-soft tissue window of the cranial abdomen in clinically normal dogs: an anatomical description using macroscopic cross-sections with vascular injection. *Anatomia, Histologia, Embryologia*. 2009;**38**: 18-22.

10. Zotti A, Banzato T, Cozzi B. Cross-sectional anatomy of the rabbit neck and trunk: comparison of computed tomography and cadaver anatomy. *Research in Veterinary Science*. 2009;**87**: 171-176.

11. Stieger-Vanegas SM, Cebra CK. Contrast-enhanced computed tomography of the gastrointestinal tract in clinically normal alpacas and llamas. *Journal of the American Veterinary Medical Association*. 2013;**242**: 254-260.

12. Beukers M, Grosso FV, Voorhout G. Computed tomographic characteristics of presumed normal canine abdominal lymph nodes. *Veterinary Radiology & Ultrasound*. 2013;**54**: 610-617.

13. Fields EL, Robertson ID, Osborne JA, Brown JC, Jr. Comparison of abdominal computed tomography and abdominal ultrasound in sedated dogs. *Veterinary Radiology & Ultrasound*. 2012;**53**: 513-517.

14. Suran JN, Wyre NR. Imaging findings in 14 domestic ferrets (*Mustela putorius furo*) with lymphoma. *Veterinary Radiology & Ultrasound*. 2013;**54**: 522-531.

15. Rossi F, Morandi F, Schwarz T. Liver, gallbladder and spleen. In: Schwarz T, Saunders J (eds): *Veterinary Computed Tomography*. Oxford: Wiley-Blackwell, 2011;297-314.

16. Beattie J. The Anatomy of the Common Marmoset (*Hapale jacchus Kuhl*). *Proceedings of the Zoological Society in London*, 1927;593-718.

17. Schwarz T. Urinary system. In: Schwarz T, Saunders J (eds): *Veterinary Computed Tomography*. Oxford: Wiley-Blackwell, 2011;331-338.

18. Morandi F. Adrenal glands. In: Schwarz T, Saunders J (eds): *Veterinary Computed Tomography*. Oxford: Wiley-Blackwell, 2011;351-356.

4.7. Tables

Table 1. Hounsfield units of the pre-contrast abdomen of the common marmoset

Organ	Number	ROI	Mean	Standard deviation	Range	
					Minimum	Maximum
Left kidney						
Cortex	8	0.03	66.35	12.74	50.40	83.50
Medulla	8	0.03	60.26	6.34	53.40	73.70
Right kidney						
Cortex	8	0.03	71.64	10.18	59.30	88.40
Medulla	8	0.03	58.04	9.17	45.43	70.70
Left adrenal	8	0.02	57.44	12.56	41.30	73.30
Right adrenal	8	0.02	56.57	9.48	42.40	69.97
Liver						
Left	8	0.10	108.04	13.60	91.70	125.80
Right	8	0.10	104.77	7.40	92.57	113.45
Gallbladder	8	0.05	45.26	6.53	34.50	53.00
Spleen	8	0.05	77.83	4.85	71.60	85.60
Fat	8	0.05	-109.78	19.52	-125.60	-67.40
Ovary						
Left	3	0.02	52.73	4.13	50.20	57.50
Right	3	0.02	55.57	4.67	50.50	59.70
Testis						
Left	2	0.02	68.56	8.74	62.38	74.74
Right	2	0.02	65.64	4.45	62.49	68.78

Table 2. Hounsfield units of the post-contrast abdomen of the common marmoset

Organ	Number	ROI	Mean	Standard deviation	Range	
					Minimum	Maximum
Left kidney						
Cortex	7	0.03	149.29	18.56	123.40	177.83
Medulla	7	0.03	167.73	40.60	113.70	246.10
Right kidney						
Cortex	7	0.03	152.73	14.67	138.70	181.92
Medulla	7	0.03	171.02	22.01	143.03	210.00
Left adrenal	7	0.02	96.96	10.69	80.60	110.60
Right adrenal	7	0.02	102.29	7.45	89.60	108.80
Liver						
Left	7	0.10	146.10	9.73	136.00	159.00
Right	7	0.10	144.09	7.27	134.40	153.30
Gallbladder	7	0.05	56.07	8.44	46.10	67.00
Spleen	7	0.05	119.55	12.75	103.20	137.24
Fat	7	0.05	-85.40	10.57	-103.40	-74.30
Ovary						
Left	3	0.02	93.62	4.96	87.90	96.85
Right	3	0.02	90.40	4.55	86.01	95.10
Testis						
Left	3	0.02	88.48	13.78	72.73	98.34
Right	3	0.02	81.92	12.38	68.26	92.40

4.8. Figures

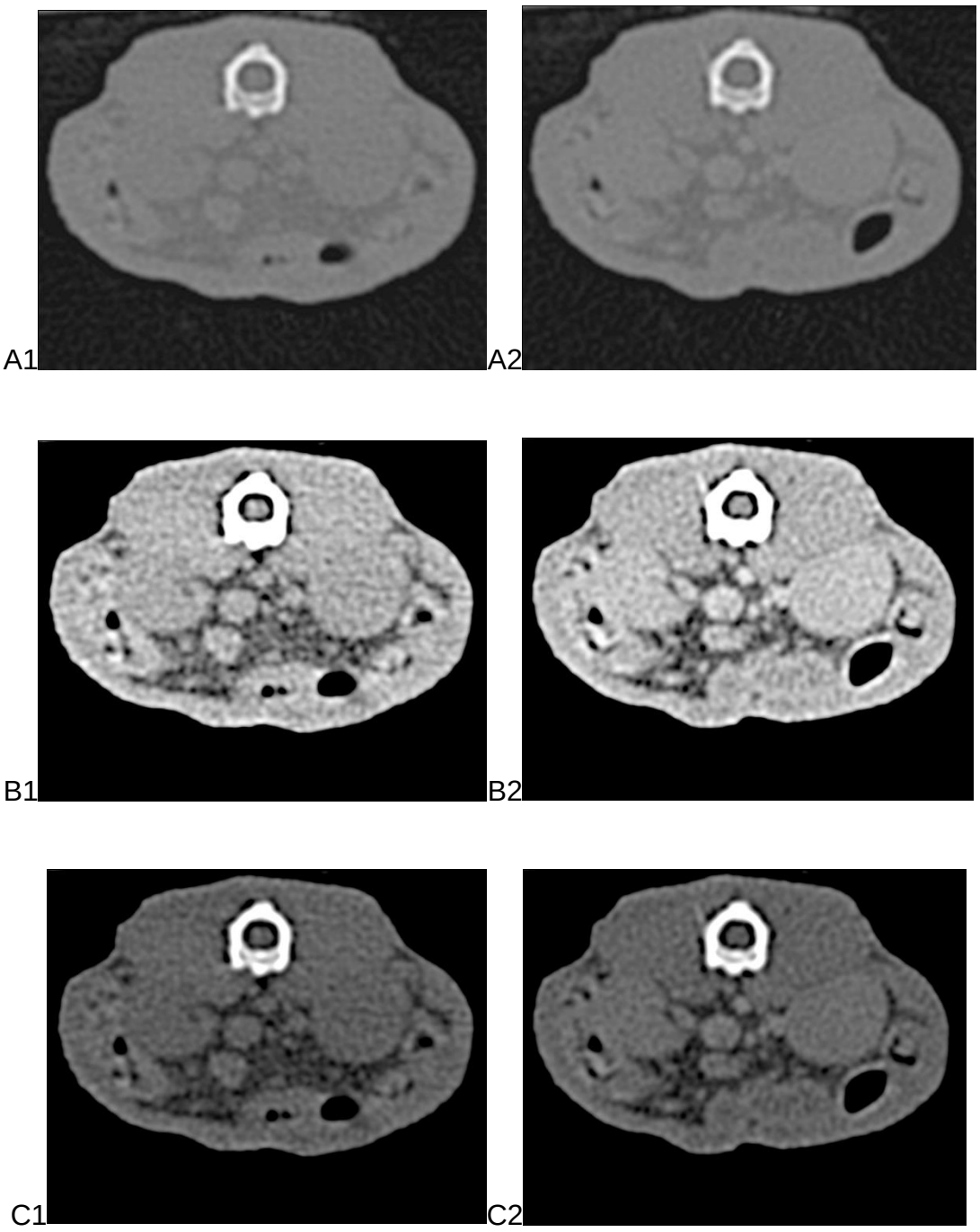

Fig. 1: Transverse images of a 21-month-old female marmoset at kidney level. Pre-contrast images on left and post-contrast images on right. Dorsal is on top and right on the left of the images. (A) Default inner ear settings (WL = 700 HU

and WW = 4000 HU) Note that no contrast could be appreciated. (B) Modified inner ear settings (WL = 50 HU and WW = 600 HU). These were considered of good quality. Contrast uptake of the blood vessels, the kidney and intestinal walls could be appreciated. (C) Modified inner ear settings (WL = 500 HU and WW =1600 HU). No additional information was gained compared to B. On the contrary, contrast could not be delineated from non-enhancing structures and images were often too dark.

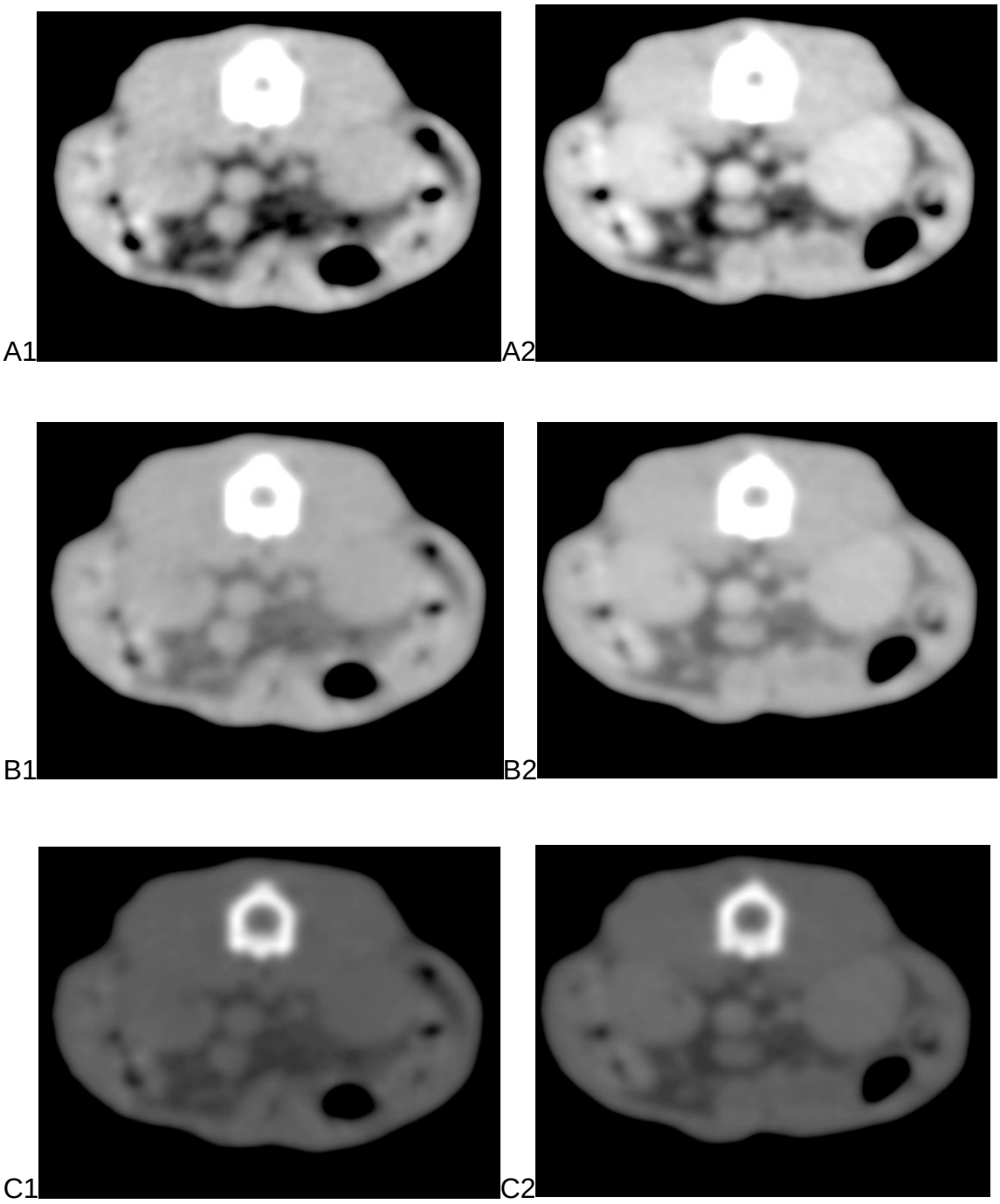

Fig. 2: Transverse images of a 21-month-old female marmoset at the kidney level. Pre-contrast images on left and post-contrast images on right. Dorsal is on top and right on the left of the images. (A) Default abdominal setting (WL=40 HU

and WW = 300 HU). These were considered to be of good quality. (B) Modified abdominal settings (WL = 50 HU and WW = 600 HU). These were considered of good quality, but not superior to A. Note that the contrast uptake could not be nicely delineated from non-enhancing structures. (C) Modified abdominal settings (WL = 500 HU and WW =1600 HU). No additional information was gained, on the contrary contrast could not be delineated from non-enhancing structures and images were too dark.

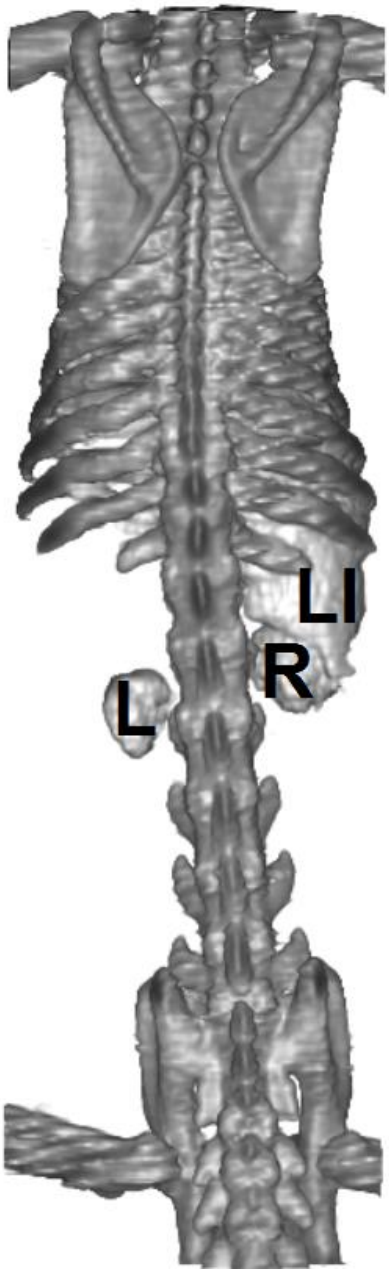

Fig. 3: Dorsal view of a 3D CT Volume rendering technique of post-contrast abdominal images. It nicely illustrates the position of the right kidney in relationship to the left. Note also the close-contact via the renal fossa with the prominent right liver as well as its far caudal extend. L = left kidney, R = right kidney, Li = liver.

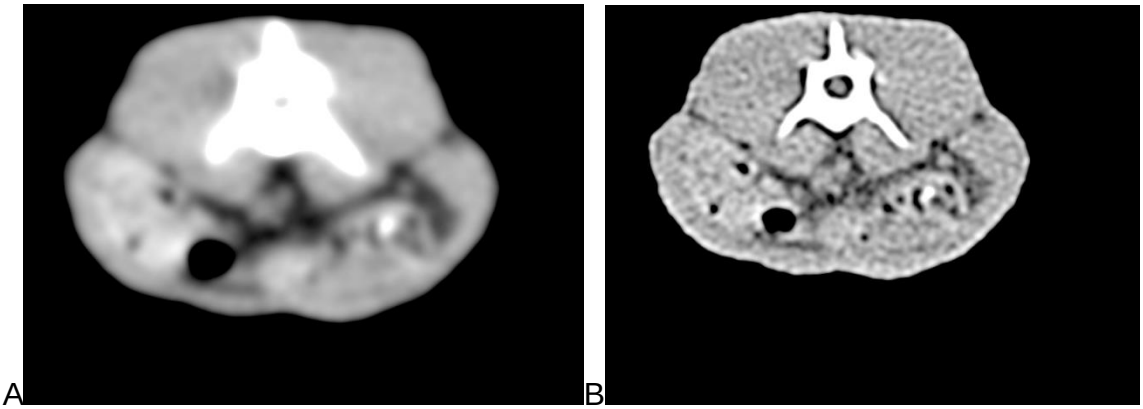

Fig. 4: Transverse (A) pre-contrast abdominal (WL = 40 HU and WW = 300 HU) and (B) inner ear pre-contrast (WL = 50 HU and WW = 600 HU) CT images of a 21-month-old female common marmoset of the caudal abdomen. Dorsal is on top and right on the left of the images. Identification of ureters on the modified inner ear pre-contrast images was possible, on abdominal settings only retrospective and not as well delineated.

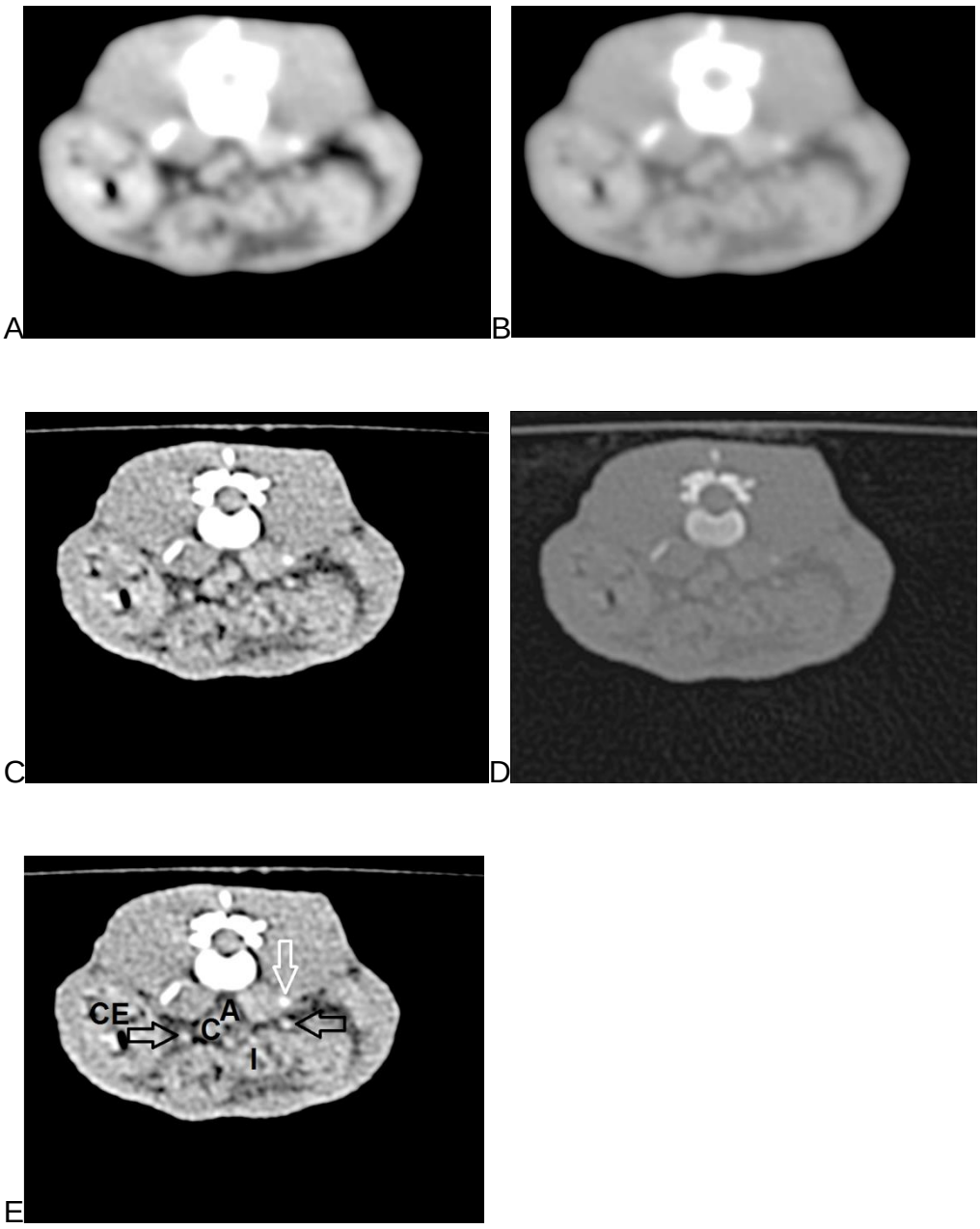

Fig. 5: Transverse post-contrast CT images of a 21-month-old female marmoset of the midabdomen with different settings. Dorsal is on top and right on the left of the images. (A) Abdomen default settings (WL = 40 HU and WW = 300 HU). (B) Modified abdominal settings (WL = 50 HU and WW = 600 HU). (C) Modified Inner Ear settings (WL = 50 HU and WW = 600 HU). (D) Inner Ear default settings (WL

= 700 HU and WW = 4000 HU). (E) Same image as (C), but with annotation. The ureters (black arrows) should not be confused with the tip of the transverse process (white arrow). A = aorta, C = caudal vena cava, CE = cecum, I = intestine. These images highlight the importance of choosing the correct settings for specific areas of interest. The ureters are best visible on a modified inner ear algorithm (C).

CHAPTER 5

ABDOMINAL COMPUTED TOMOGRAPHIC ATLAS IN CLINICALLY NORMAL COMMON MARMOSETS (*Callithrix jacchus*) AND COMPARISON OF COMPUTED TOMOGRAPHY TO OTHER IMAGING MODALITIES

5.1. Introduction

The common marmoset is an arboreal small New World primate originating from South America, but is a commonly kept pet in certain parts of the world such as the Republic of South Africa. Additionally, the common marmoset is frequently used as an animal model for neuroscience[1,2] and to examine disease.[3,4]

Survey radiography and abdominal ultrasonography (US) have been considered as the primary imaging modalities for abdominal evaluation in dogs and cats, however with the advent of computed tomography (CT) an increasing number of studies are being performed to compare CT with other diagnostic imaging modalities such as radiography and ultrasonography for small animals.[5-16] In instances of acute abdominal signs diagnostic imaging plays a vital role for guidance of appropriate medical or surgical intervention. A study group compared multiple imaging modalities such as radiography, ultrasonography and CT in dogs with acute abdominal signs and found that accuracy for differentiation of surgical versus non-surgical conditions was high for all modalities.[5] As CT protocols are becoming more refined,[17] there is a need to clinically reassess the role of CT in abdominal imaging of the small animal. One recent study comparing US with CT in sedated dogs found that CT was only superior to US in animals weighing 25 kg or more.[7] To the best of the authors' knowledge no study has been done comparing different imaging modalities in the common marmoset or in any exotic species concerning abdominal imaging.

Normal abdominal ultrasonographic[18] and radiographic[19] anatomy of the common marmoset as well as the thoracic[20] anatomy via computed tomography has been described. The technique for abdominal CT of the marmoset[21] has also been established, although representative anatomy images were not published. The same article highlighted the importance of critically assessing and adapting standard small animal CT protocols for exotics because of species-specific anatomy. A high frequency algorithm with edge enhancement proved to be particularly beneficial for the evaluation of thoracic[20] and to a lesser degree abdominal[21] CT in clinically normal common marmosets. Since the reference range of Hounsfield units for abdominal organs varied from that of small animals, the viewing and display settings should also be adapted accordingly.[21]

The aims of this study were to provide an abdominal CT atlas in clinically normal common marmosets to establish similar baseline studies as have been performed in dogs[22,23] and cats[24] and to compare abdominal CT in the common marmoset with other diagnostic imaging modalities, such as radiography and US.

5.2. Materials and methods

This prospective study was approved by the University of Pretoria Ethics Committee.

Animals: Eight unrelated mature male (n=5) and non-pregnant female (n=3) marmosets (mean +/- SD age, 23.6 +/- 14.5 months; range, 12 to 48 months)

were included in this CT study and 3/8 had radiographs taken at the same time. They were anaesthetized with Isoflurane inhalation (Isofor, Safe Line Pharmaceuticals, Florida, South Africa) for both procedures. All animals were clinically healthy based on physical examination and routine haematological and biochemical analysis. Food was withheld for 12 hours, but water was accessible shortly prior to the procedures.

Diagnostic Imaging: A dual slice helical CT scanner (Siemens Emotion Duo, Siemens, Erlangen, Germany) was used to acquire transverse images of the whole body using a craniocaudal scan direction from cranial to the diaphragm to caudal to the pelvis with 1 mm collimation and a pitch of 1.5.

For the post-contrast study, 1 ml/kg of Omnipaque 350 mg I/ml (Amersham Health (Pty) Ltd, Constantia Park, South Africa) with a 0.05 ml chaser was injected manually into the femoral vein via intravenous (i.v.) catheter with image acquisition directly afterwards (venous phase).

The images were viewed with a high frequency algorithm with edge enhancement (window level (WL) = 700 HU and window width (WW) = 4000 HU) and WL = 50 HU and WW = 600 HU) as well as soft tissue windows (WL = 40 HU and WW = 300 HU and WL = 50 and WW = 600 HU).

Additionally right lateral and ventrodorsal (VD) abdominal radiography was performed in three animals following the CT examination.

Evaluation: The CT images were assessed by one examiner (WMdP) using dedicated software (OsiriX open Source™ Version 3.9.1., Osirix Foundation, Geneva, Switzerland). The anatomy was correlated with findings from anatomy studies and literature[25] and representative cross-sectional images were chosen to illustrate the abdominal CT anatomy. The visibility and information gained from CT images were compared to radiographic findings of three animals using an organ system approach. In the discussion, these were correlated to radiographic[19] and ultrasonographic[18] findings of another study population done by the main investigator as well as other reported literature.

5.3. Results

Contrast administration was well tolerated in all animals and no adverse reactions were observed.

Representative cross-sectional images were chosen from different animals illustrating the abdominal CT anatomy of clinically normal common marmosets. Images follow the scan direction from cranial to caudal to the kidney level. Concerning the gastrointestinal tract, the image order follows an oral to aboral approach.

Organ systems are discussed comparing radiography versus survey CT findings, followed by additional information gained by post-contrast CT images.

Radiographically, the last ribs were difficult to detect and in 2/3 animals marked asymmetry of the right versus left rib (Fig. 1) was noticed, whereas on CT the

number of ribs could consistently be determined to be 13 in all 3 cases and ribs were much more symmetrical. Furthermore CT assisted in detection of vestigial ribs which pointed caudally in contrast to the cranially pointing transverse processes of lumbar vertebrae. Although the vertebral number could be consistently and reliably determined using CT, counting vertebrae was more time consuming and cumbersome than using radiographs, since multi-plane reconstructions and 3D-reconstructions proved to be most helpful. One animal had a transitional sacral vertebra, which was easier to appreciate radiographically. Post-contrast CT did not provide any additional information concerning the skeletal system.

Radiographically, serosal abdominal detail was poor in all 3 animals despite good survey CT abdominal detail in all 8 animals.

The prominence of the right liver could easily be appreciated radiographically; however the caudal margin could often not reliably be determined. The gallbladder was not visible radiographically. Although motion artifacts could affect the cranial abdomen due to the close proximity to the diaphragm, the liver and gallbladder were well visualized on survey CT (Figs. 2-3). Post-contrast CT resulted in marked contrast uptake of the liver without contrast uptake of the gallbladder or its wall, enhancing overall visibility of the gallbladder. Hepatic vasculature could be appreciated.

The spleen and adrenal glands could not be identified radiographically, but were easily visible on survey CT (Figs. 4-5). Post-contrast CT facilitated easier identification and better delineation of the right adrenal gland. A landmark

approach using vasculature for identification of the adrenal glands was not necessary.

Radiographically both kidneys were difficult to detect on the VD view, and often not visible on laterals. The right kidney was cranial to the left kidney in 1/3 animals on VD radiographs, and caudal in 2/3. This was consistent with the CT findings in the same animals. Post-contrast did enhance the kidneys (Figs. 6-7) and also enabled detection of the ureters. Ease of detection of the urinary bladder depended on filling status on CT, but could never be detected radiographically. Post-contrast images did not provide additional information concerning the urinary bladder.

Radiographically the GIT could often only be differentiated due to its luminal content. Individual GIT identification such as stomach, duodenum and cecum or even small versus large intestine was not consistently possible. On survey CT (Figs. 8-11) the stomach and cecum were the easiest to identify. Post-processing and 3D reconstructions assisted in correct identification of individual GIT components. On post-contrast, the GIT walls enhanced nicely differentiating them from luminal fluid. No individual wall layering could be determined.

Lymph nodes were inconsistently identified on CT (Fig. 9), but never radiographically. Post-contrast CT was helpful to identify lymph nodes due to their close proximity to adjacent enhanced vasculature.

The ovaries and uterus could more reliably be detected on post-contrast CT, but never radiographically.

The pancreas and prostate could not be reliably identified on CT or radiographs.

No vascular structures could be identified radiographically, whereas on CT some vessels such as the caudal vena cava, aorta and renal veins could be identified, particularly if surrounded by fat. Contrast CT and 3D CT reconstructions assisted in identifying major blood vessels.

5.4. Discussion

Depending on the clinical presentation, US and radiography constituted the modalities of choice for abdominal imaging in small animal patients, with certain examiner and institute preference for the first choice modality. However, recent human literature pointed out that abdominal radiography was of limited value in certain abdominal presentations,[26,27] since it missed major pathology or led to incorrect diagnosis in a high percentage of cases. Therefore CT has become first choice imaging modality in humans for certain abdominal presentations, such as the acute abdomen. Similarly more studies have investigated and compared different imaging modalities in small animals.[5-15] The purpose of this paper was to provide an abdominal CT atlas as a reference and to compare abdominal CT in the common marmoset with other diagnostic imaging modalities, such as radiography and US. Inherent imaging characteristics such as topographic versus tomographic characteristics will only be briefly mentioned, since the same would apply for small animals and have been extensively discussed elsewhere.

The marked physical and physiological differences that exist between exotic animals and small animals and differences in how procedures are performed

influence the choice of different imaging modalities. Anesthesia or sedation is an important decision criteria for small animals, since often only required for CT in small animals. This is not the case in the common marmoset and many other small exotics, which are often anesthetised for any diagnostic imaging procedure. In small exotics such as the common marmoset, whole body imaging is often the standard procedure for radiography and CT in contrast to dogs and cats. Hence in exotic imaging, CT and radiography have the advantage of detecting extra-abdominal lesions (particularly thoracic and skeletal disease) which would be missed by abdominal ultrasound. However, additional thoracic or skeletal imaging could be performed if clinically indicated.

Computed tomography versus radiography: When comparing CT with radiography in the common marmoset, inherent advantages of CT included its post-processing ability, reconstruction in all imaging planes as well as 3D-reconstruction and tomographic ability, and its increased low contrast resolution. Although the actual CT scan time took less than 10 minutes, patient preparation including i.v. catheter placement and post-processing as well as reporting made CT more time consuming overall in comparison to radiography. Though i.v. injection was well tolerated and no adverse reaction was observed, it must be emphasized that i.v. catheter placement could be challenging in this species – even for an experienced specialist. Post-contrast CT assisted in identification and delineation of organs and was felt to increase examiner confidence level;

however a majority of difference between CT and radiography were independent of contrast administration.

The small number of common marmosets (particularly for radiography) could be considered a limitation of this study. However, radiographic findings such as poor serosal abdominal detail and a prominent right liver were very consistent and correlated well with a previous study done by the primary investigator in 17 common marmosets,[19] emphasizing the difference to small animals. The author found it important to compare radiography and CT in the same species and not just to compare them to a different one.

This study found that radiography could incorrectly record the number of ribs - and thus thoracic vertebrae – in contrast to CT. Furthermore other features of a transitional vertebra such as vestigial ribs or cranially orientated transverse processes of the lumbar vertebrae could be recognized on CT, but not radiographically. Hence any radiographic study classifying thoracic and lumbar vertebra should be critically assessed. Although an overview of the skeletal system was often easier radiographically. Cost and availability would be in favor of radiography.

In comparison to small animals the limitations of abdominal radiography were accentuated in the common marmoset by the generally poor serosal abdominal detail. This hampered identification and the margination of major abdominal organs. Poor serosal abdominal detail therefore must not be misinterpreted as ascites.[19] On CT the abdominal contrast was good in the same animals (3/3) with fat providing the contrast.

In contrast to small animals, the spleen and urinary bladder could not be seen radiographically, but were visible on survey CT with i.v. contrast improving identification and assessment of the spleen. Radiographically, the gastrointestinal system could often only be identified because of its luminal gas content versus serosal margin on CT. Wall thickness cannot be assessed on survey radiographs, but has been reported on CT.[28] Some of the limitations of radiography could be overcome with gastrointestinal (barium or iodine), urinary and lymphatic contrast studies. However, these would all constitute additional time consuming specific contrast procedures which thus represent no benefit when compared to CT. These contrast procedures, if desired, could also be done for CT. The pancreas could not be assessed on CT or radiographs. The lymph nodes were not visible radiographically, but could occasionally be seen on CT, with i.v. contrast once again assisting. Similar to small animals the ureters, lymph nodes, abdominal blood vessels, pancreas, gallbladder, ovaries, uterus and adrenal glands were not visible radiographically.

Computed tomography versus US: Based on clinical experience and newer literature, US is often considered the imaging modality of choice for evaluating small animal patients with abdominal disease.[29, 30] A previous US study of 17 common marmosets showed that ultrasound provided visualization of not only the same, but additional anatomic features compared with CT.[18] Since US is a dynamic modality, additional information such as peristalsis and motility was possible. Furthermore, US-guided cystocentesis and fine needle aspiration of

organs and lesions could be performed in the common marmoset as well (personal observation Dr. du Plessis). Spectral Doppler enabled easy investigation of blood vessels giving valuable information concerning flow pattern and velocity.[18] Additionally, using Colour or Power Doppler information concerning vascularisation of organs and lesions could be obtained.

As previously stated, some limitations of CT could be overcome with additional contrast procedures such as gastrointestinal (barium or iodine), urinary and lymphatic contrast studies. However, ultrasound would circumvent their necessity. Ultrasonography also provided much more morphologic information than CT. Radiation safety and exposure should also be a decision criteria. Reproductive related clinical diseases are frequent in the common marmoset, including pregnancy, since they are often not spayed and kept for breeding purposes. However pregnancy would be a contra-indication for CT. This poses another limitation for the use of abdominal CT in the common marmoset.

Due to time limitations, the US study only looked at the GIT of 8/20 common marmosets. However, the classical 5-layered gastrointestinal wall, motility, peristalsis and luminal content could easily be assessed unlike in the CT study. In a CT study of the GIT of dogs, wall layering could only be determined in 24% of the 77.7% i.v. contrast enhanced gastrointestinal segments, with no distinction of individual layers as described in sonographic evaluations.[28] The gas in the cecum did not hamper evaluation of the abdomen in the common marmoset, and could be easily avoided by using a more lateral approach on US. On US the duodenum could be easily identified and continuously scanned from the pylorus.

Concerning the kidneys using US, clear cranial demarcation was always possible and a high percentage also showed corticomedullary distinction, even though often poor. Using Doppler, additional information such as the resistive index could be determined. Ureteral jets could also be observed (personal observation Dr. du Plessis). The urinary bladder could be seen on both modalities, with US being able to assess the urinary bladder wall and assisting in cystocentesis (personal observation Dr. du Plessis)

The spleen could easily be seen on both modalities, once different echogenicity and more dorsal location compared to small animals was appreciated by the examiner. Normal lymph nodes could only occasionally be seen on CT, but did not form part of the US study. However, enlarged lymph nodes could be easily seen on US in the common marmoset for example in cases of reactive lymphadenopathy with enteritis (personal observation Dr. du Plessis). This would be similarly expected for CT.

Concerning the ovaries and uterus, the benefits of US have been described also using contrast US[31] or in similar species such as the tamarind.[32] The use of US for pregnancy evaluations and complications is commonly applied in practice (personal observation Dr. du Plessis).

The adrenal glands served as an excellent example for the benefit of US over CT for the abdomen in the common marmoset. On US the adrenal glands were very easily detectable in the common marmoset without a landmark approach unlike in small animals. In the study of 17 marmosets,[18] all adrenal glands were easily identified and the corticomedullary distinction was clearly visible (Fig. 12). In this

CT study the adrenal glands could be identified, but contrast medium application assisted in anatomic identification dramatically (particularly of the right). Even with contrast no corticomedullary distinction was possible, and the overall information gained from CT was not believed to be superior to US.

After i.v. contrast some information concerning the intrahepatic vasculature became available, however close vicinity to the diaphragm made this area susceptible for motion artifacts with CT. Hepatic and portal vasculature could easily be assessed as well as more morphologic information obtained on US. Using 3D CT-reconstruction could provide more complex and overall information and multi-phase CT has been reported to be 5.5 times more likely to correctly ascertain the presence or absence of PSS compared to abdominal US,[33] however PSS are not reported in the literature for common marmosets. Not only could the gall bladder be easily detected on US, but its wall assessed and its multi-lobed appearance clearly seen including the cystic ducts, whereas on CT the gallbladder itself could only be appreciated. An advantage of CT would be the possibility to establish hepatic volumetric information.[34]

One inherent disadvantage of US is that it is highly operator dependent and exotic experience is needed, therefore there is greater potential for variation in abdominal US and less repeatability, whereas CT and radiography eliminate some of these variables. Ultrasonography has also been reported to overestimate true size of cystoliths.[9]

Adequate equipment with high resolution frequency probes (at least 7.5 MHz, but ideally higher) and small contact surface should be used for US. Additionally in

certain clinical scenarios with lots of gas in the GIT, preference should be given to radiography or CT. Due to their high metabolic rate, the common marmoset should always be positioned on a heat pad and warmed US gel should be used to minimize heat loss to avoid further compromise (Fig. 13). Depending on the clinical presentation, dorsal recumbency might be contra-indicated. Since US is performed under anesthesia in the common marmoset, the decreased patient compliance experienced in small animals with an acute abdomen is not applicable.

A recent study comparing CT to US in sedated dogs[6] only found significant improved information on CT in heavier animals (more than >25 kg). Conversely, the small size of the common marmoset has significant limitations using dual slice CT. This once again emphasized that information gained from small animals does not extrapolate well to exotics. With higher multi-slice CT this limitation should be further overcome, however 16-slice CTs and higher are still more commonly seen in academic environments.

In summary, since the imaging decision is multi-factorial and highly dependent on individual case scenario, variables such as cost, time, experience of modality and species, emotional value, availability and accessibility of equipment will be important decision criteria in real case scenarios and realistic clinical settings. Under ideal circumstances, US is recommended as the screening tool of choice for the abdomen in the common marmoset, with CT being considered in cases when further diagnostic work-up is required. Radiography will still play an important role as baseline imaging modality, particularly since done as whole

body radiograph in the common marmoset, providing simultaneous information about the thorax and skeletal system; however its limitations must be considered.

5.5. Conclusion

Abdominal CT rendered additional information compared to abdominal radiography; however ultrasound should still be considered the screening modality of choice for abdominal imaging in the common marmoset. In cases where further work-up would be required or in certain clinical presentations, CT would be recommended as an additional diagnostic imaging modality and should always be combined with i.v. contrast.

5.6. References

1. Kishi N, Sato K, Sasaki E, Okano H. Common marmoset as a new model animal for neuroscience research and genome editing technology. *Development, Growth & Differentiation*. 2014;**56**: 53-62.

2. Okano H, Hikishima K, Iriki A, Sasaki E. The common marmoset as a novel animal model system for biomedical and neuroscience research applications. *Seminars in Fetal & Neonatal Medicine*. 2012;**17**: 336-340.

3. Lever MS, Stagg AJ, Nelson M, Pearce P, Stevens DJ, Scott EA, et al. Experimental respiratory anthrax infection in the common marmoset (*Callithrix jacchus*). *International Journal of Experimental Pathology*. 2008;**89**: 171-179.

4. Nelson M, Loveday M. Exploring the innate immunological response of an alternative nonhuman primate model of infectious disease; the common marmoset. *Journal of Immunology Research*. 2014;**2014**: 913632.

5. Shanaman MM, Schwarz T, Gal A, O'Brien RT. Comparison between survey radiography, B-Mode ultrasonography, contrast-enhanced ultrasonography and contrast-enhanced multi-detector computed tomography findings in dogs with acute abdominal signs. *Veterinary Radiology & Ultrasound. 2013;**54**:591-604.*

6. Fields EL, Robertson ID, Osborne JA, Brown JC, Jr. Comparison of abdominal computed tomography and abdominal ultrasound in sedated dogs. *Veterinary Radiology & Ultrasound.* 2012;**53**: 513-517.

7. Taeymans O, Penninck DG, Peters RM. Comparison between clinical, ultrasound, CT, MRI, and pathology findings in dogs presented for suspected thyroid carcinoma. *Veterinary Radiology & Ultrasound*. 2013;**54**: 61-70.

8. Alexander K, Joly H, Blond L, D'Anjou MA, Nadeau ME, Olive J, et al. A comparison of computed tomography, computed radiography, and film-screen radiography for the detection of canine pulmonary nodules. *Veterinary Radiology & Ultrasound*. 2012;**53**: 258-265.

9. Byl KM, Kruger JM, Kinns J, Nelson NC, Hauptman JG, Johnson CA. In vitro comparison of plain radiography, double-contrast cystography,

ultrasonography, and computed tomography for estimation of cystolith size. *American Journal of Veterinary Research*. 2010;**71**: 374-380.

10. Ober CP, Jones JC, Larson MM, Lanz OI, Werre SR. Comparison of ultrasound, computed tomography, and magnetic resonance imaging in detection of acute wooden foreign bodies in the canine manus. *Veterinary Radiology & Ultrasound*. 2008;**49**: 411-418.

11. Marolf A, Blaik M, Ackerman N, Watson E, Gibson N, Thompson M. Comparison of computed radiography and conventional radiography in detection of small volume pneumoperitoneum. *Veterinary Radiology & Ultrasound*. 2008;**49**: 227-232.

12. Esterline ML, Radlinsky MG, Biller DS, Mason DE, Roush JK, Cash WC. Comparison of radiographic and computed tomography lymphangiography for identification of the canine thoracic duct. *Veterinary Radiology & Ultrasound*. 2005;**46**: 391-395.

13. Nemanic S, Nelson NC. Ultrasonography and noncontrast computed tomography of medial retropharyngeal lymph nodes in healthy cats. *American Journal of Veterinary Research*. 2012;**73**: 1377-1385.

14. Saunders JH, van Bree H. Comparison of radiography and computed tomography for the diagnosis of canine nasal aspergillosis. *Veterinary Radiology & Ultrasound*. 2003;**44**: 414-419.

15. Robben JH, Pollak YW, Kirpensteijn J, Boroffka SA, van den Ingh TS, Teske E, et al. Comparison of ultrasonography, computed tomography, and

single-photon emission computed tomography for the detection and localization of canine insulinoma. *Journal of Veterinary Internal Medicine*. 2005;**19**: 15-22.

16. King AM, Weinrauch SA, Doust R, Hammond G, Yam PS, Sullivan M. Comparison of ultrasonography, radiography and a single computed tomography slice for fluid identification within the feline tympanic bulla. *Veterinary Journal*. 2007;**173**: 638-644.

17. Fields EL, Robertson ID, Brown JC, Jr. Optimization of contrast-enhanced multidetector abdominal computed tomography in sedated canine patients. *Veterinary Radiology & Ultrasound*. 2012;**53**: 507-512.

18. Wagner WM, Kirberger RM. Transcutaneous ultrasonography of the abdomen in the normal common marmoset (*Callithrix jacchus*). *Veterinary Radiology & Ultrasound*. 2005;**46**: 251-258.

19. Wagner WM, Kirberger RM. Radiographic anatomy of the thorax and abdomen of the common marmoset (*Callithrix jacchus*). *Veterinary Radiology & Ultrasound*. 2005;**46**: 217-224.

20. du Plessis WM, Groenewald HB, Elliot D. Computed tomographic thoracic anatomy in eight clinically normal common marmosets (*Callithrix jacchus*). 2015, submitted for publication.

21. du Plessis WM, Groenewald HB, Elliot D. Computed tomography of the abdomen in eight clinically normal common marmosets (*Callithrix jacchus*). 2015, submitted for publication.

22. Teixeira M, Gil F, Vazquez JM, Cardoso L, Arencibia A, Ramirez-Zarzosa G, et al. Helical computed tomographic anatomy of the canine abdomen. *Veterinary Journal*. 2007;**174**: 133-138.

23. Rivero MA, Vazquez JM, Gil F, Ramirez JA, Vilar JM, De Miguel A, et al. CT-soft tissue window of the cranial abdomen in clinically normal dogs: an anatomical description using macroscopic cross-sections with vascular injection. *Anatomia, Histologia, Embryologia*. 2009;**38**: 18-22.

24. Samii VF, Biller DS, Koblik PD. Normal cross-sectional anatomy of the feline thorax and abdomen: comparison of computed tomography and cadaver anatomy. *Veterinary Radiology & Ultrasound*. 1998;**39**: 504-511.

25. Beattie J. The Anatomy of the Common Marmoset (*Hapale jacchus Kuhl*). *Proceedings of the Zoological Society in London*, 1927;593-718.

26. Kellow ZS, MacInnes M, Kurzencwyg D, Rawal S, Jaffer R, Kovacina B, et al. The role of abdominal radiography in the evaluation of the nontrauma emergency patient. *Radiology*. 2008;**248**: 887-893.

27. van Randen A, Lameris W, Luitse JS, Gorzeman M, Hesselink EJ, Dolmans DE, et al. The role of plain radiographs in patients with acute abdominal pain at the ED. *The American Journal of Emergency Medicine*. 2011;**29**: 582-589.

28. Hoey S, Drees R, Hetzel S. Evaluation of the gastrointestinal tract in dogs using computed tomography. *Veterinary Radiology & Ultrasound*. 2013;**54**: 25-30.

29. Sharma A, Thompson MS, Scrivani PV, Dykes NL, Yeager AE, Freer SR, et al. Comparison of radiography and ultrasonography for diagnosing small-intestinal mechanical obstruction in vomiting dogs. *Veterinary Radiology & Ultrasound*. 2011;**52**: 248-255.

30. Tyrrell D, Beck C. Survey of the use of radiography vs. ultrasonography in the investigation of gastrointestinal foreign bodies in small animals. *Veterinary Radiology & Ultrasound*. 2006;**47**: 404-408.

31. Hastings JM, Morris KD, Allan D, Wilson H, Millar RP, Fraser HM, et al. Contrast imaging ultrasound detects abnormalities in the marmoset ovary. *American Journal of Primatology*. 2012;**74**: 1088-1096.

32. Kuederling I, Heistermann M. Ultrasonographic and hormonal monitoring of pregnancy in the saddle back tamarin, Saguinus fuscicollis. *Journal of Medical Primatology*. 1997;**26**: 299-306.

33. Kim SE, Giglio RF, Reese DJ, Reese SL, Bacon NJ, Ellison GW. Comparison of computed tomographic angiography and ultrasonography for the detection and characterization of portosystemic shunts in dogs. *Veterinary Radiology & Ultrasound.* 2013;**54**:569-574.

34. Stieger SM, Zwingenberger A, Pollard RE, Kyles AE, Wisner ER. Hepatic volume estimation using quantitative computed tomography in dogs with portosystemic shunts. *Veterinary Radiology & Ultrasound*. 2007;**48**: 409-413.

5.7. Figures

A 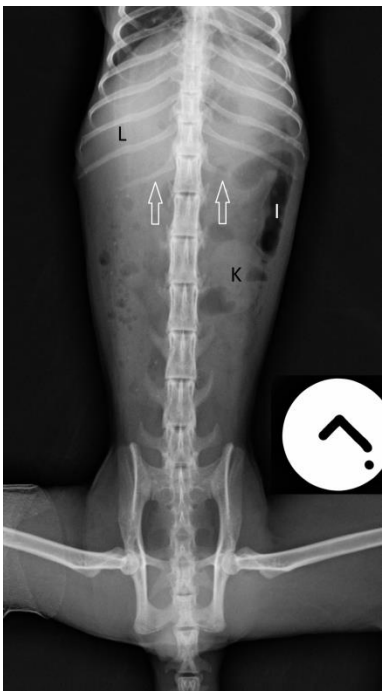

B 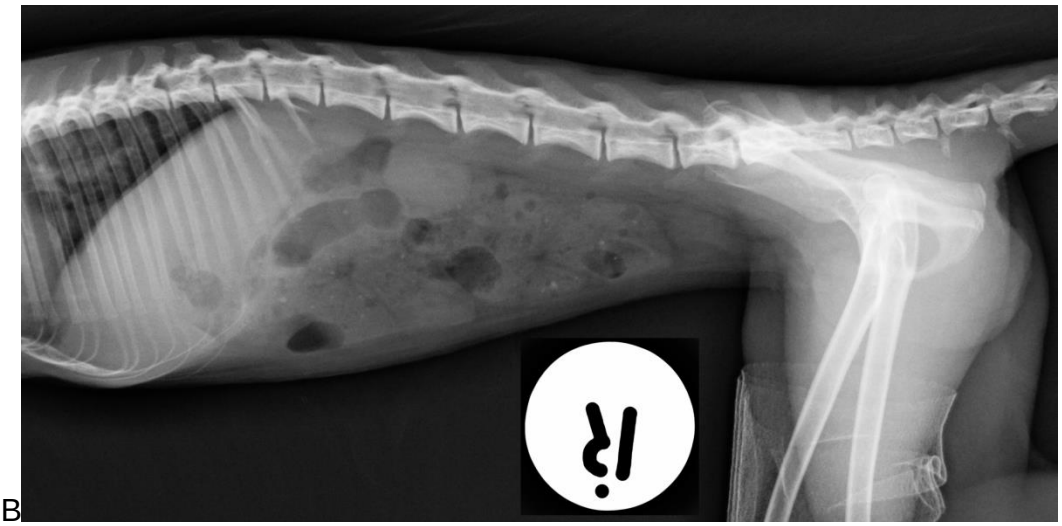

Fig. 1: Right lateral (A) and ventrodorsal (B) survey radiographs of a 21-month-old female marmoset (same animal as CT images of Figs. 4-7). The poor serosal abdominal detail is typical for the common marmoset as well as the prominent right liver (L). Intestines (I) are often only detectable because of luminal content (here gas/fecal balls). Both kidneys (K) are not clearly visible. The spleen,

adrenal glands, blood vessels, cecum, bladder, spleen, ovaries and uterus are not visible contrary to CT. Note the marked asymmetry of the last rib pair (white arrows), which could be easily misinterpreted as transitional vertebra. On CT both ribs were easily visible and of fairly symmetric appearance.

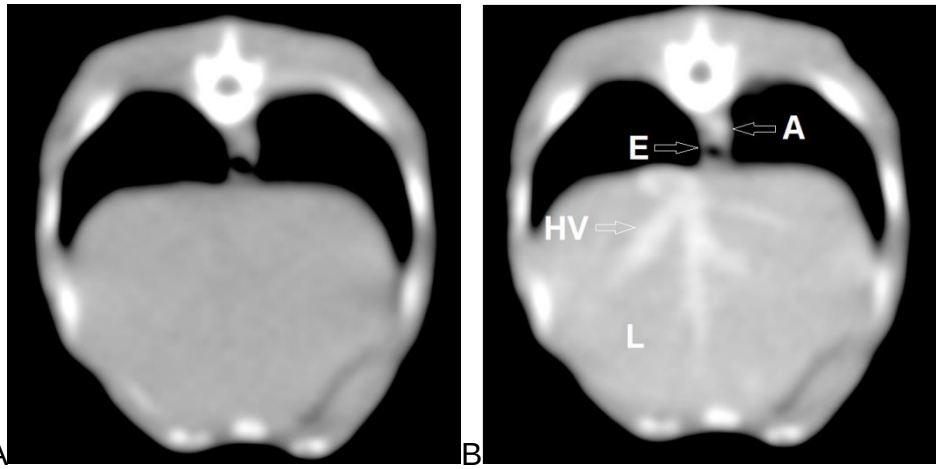

Fig. 2: Transverse CT images of the liver (L) of a 16-month-old male marmoset at the level of T10. Dorsal is on top and right on the left of the image. (A) Pre- and (B) post-contrast images displayed in a soft tissue window (WL = 50 and WW = 600). Note that the terminal esophagus was often gas filled (E). A = Aorta. HV = hepatic vein.

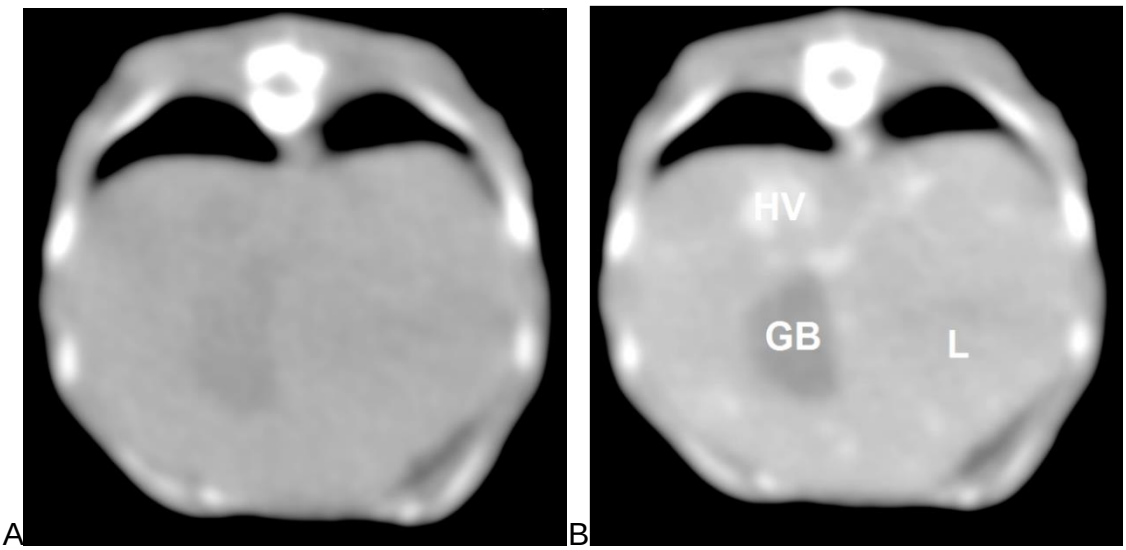

Fig. 3: Transverse CT images of the liver (L) of a 16-month-old male marmoset at the level of T11. Dorsal is on top and right on the left of the image. (A) Pre- and (B) post-contrast images displayed in a soft tissue window (WL = 50 and WW = 600). The gallbladder (GB) is much better delineated on post-contrast images since the liver takes up contrast markedly, whereas the GB does not. HV = hepatic veins.

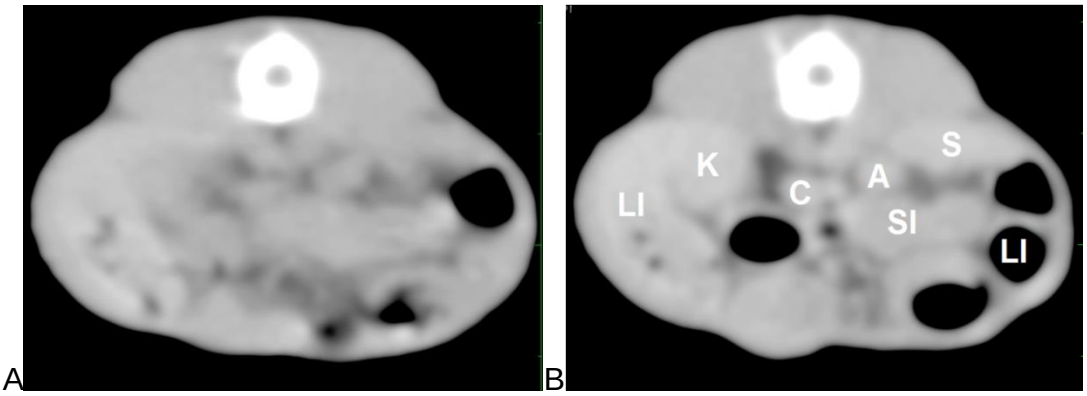

Fig. 4: Transverse CT images of the spleen (S) of a 21-month-old female marmoset at the level of T13-L1. Dorsal is on top and right on the left of the image. (A) Pre- and (B) post-contrast images displayed in a soft tissue window (WL = 50 and WW = 600). S = spleen, LI = large intestine. SI = small intestine. C = caudal vena cava. A = left adrenal gland. K = right kidney.

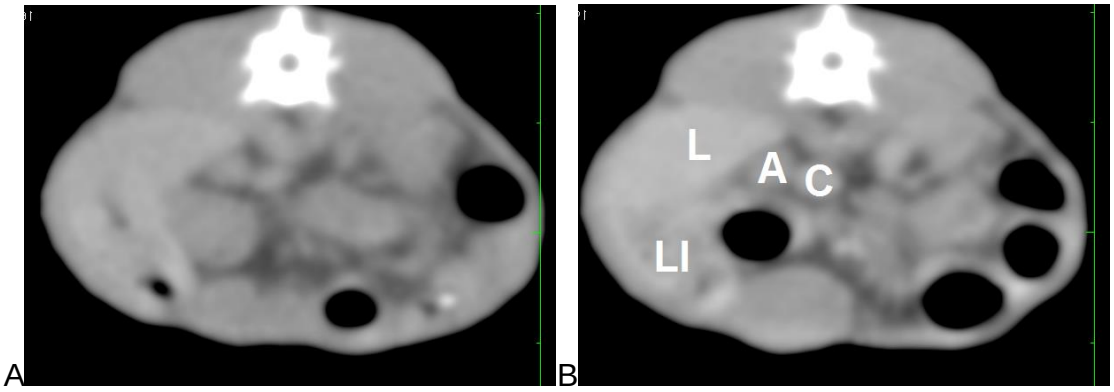

Fig. 5: Transverse CT images of the right adrenal gland (A) of a 21-month-old female marmoset at the level of T13. Dorsal is on top and right on the left of the image. (A) Pre- and (B) post-contrast images displayed in a soft tissue window (WL = 50 and WW = 600). Due to close proximity to the right kidney, contrast assisted in identification and clear demarcation of the right adrenal gland. Even on post-contrast images no corticomedullary distinction present. L = liver. LI = large intestine. C = caudal vena cava.

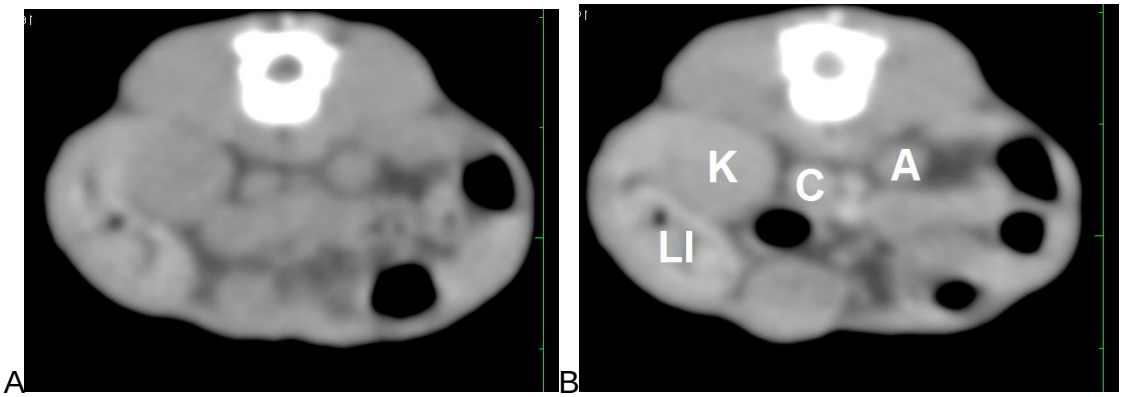

Fig. 6: Transverse CT images of the left adrenal gland (A) of a 21-month-old female marmoset at the level of cranial L1. Dorsal is on top and right on the left of the image. (A) Pre- and (B) post-contrast images displayed in a soft tissue window (WL = 50 and WW = 600). The left adrenal gland could always nicely be identified. C = caudal vena cava. K = right kidney. LI = large intestine.

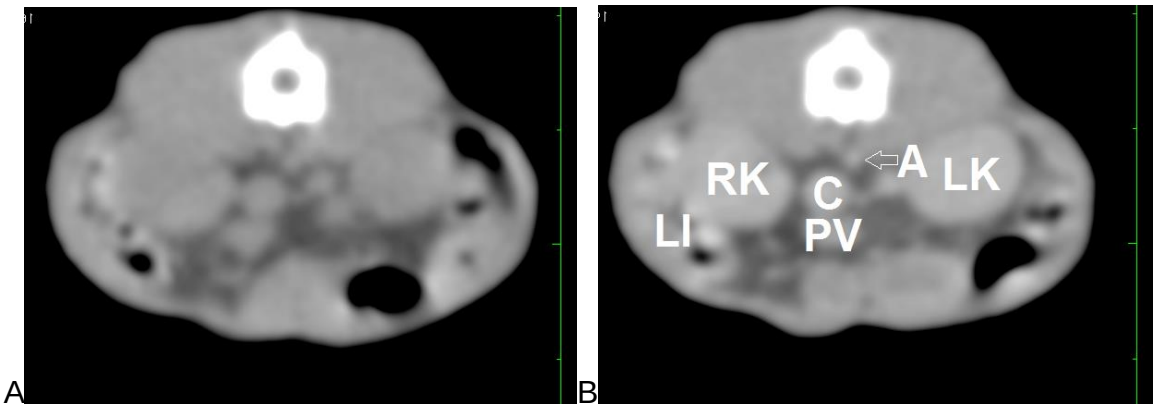

Fig. 7: Transverse CT images of both kidneys of a 21-month-old female marmoset at the level of caudal L1. Dorsal is on top and right on the left of the image. (A) Pre- and (B) post-contrast images displayed in a soft tissue window (WL = 50 and WW = 600). A = Aorta. C = Caudal vena cava. PV = portal vein. RK = right kidney. LK = left kidney.

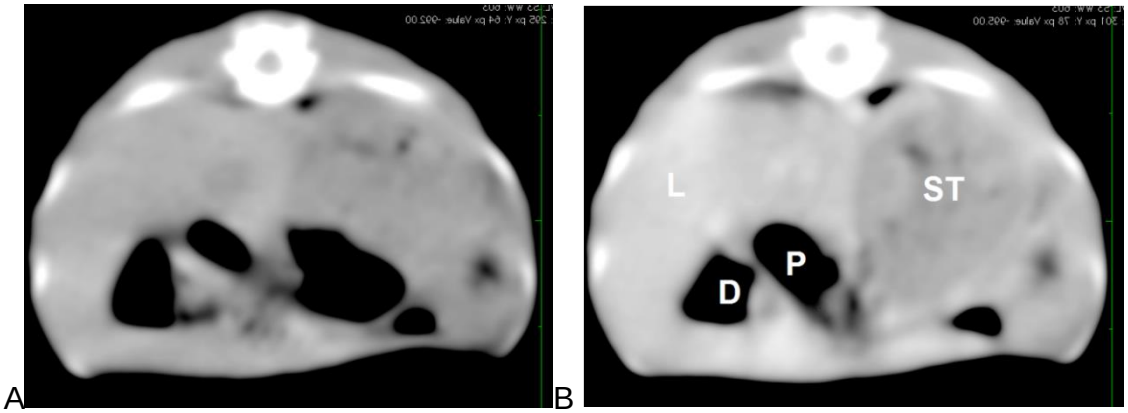

Fig. 8: Transverse CT images of the stomach (ST) of a 48-month-old male marmoset at the level of T12-13. Dorsal is on top and right on the left of the image. (A) Pre- and (B) post-contrast images displayed in a soft tissue window (WL = 50 and WW = 600). P = pylorus. D = duodenum. L = liver. The right liver is very prominent. The pylorus is gas filled and just extends to the right of the midline. On post-contrast the fluid filled gastric content can be better distinguished from the contrast enhanced gastric wall.

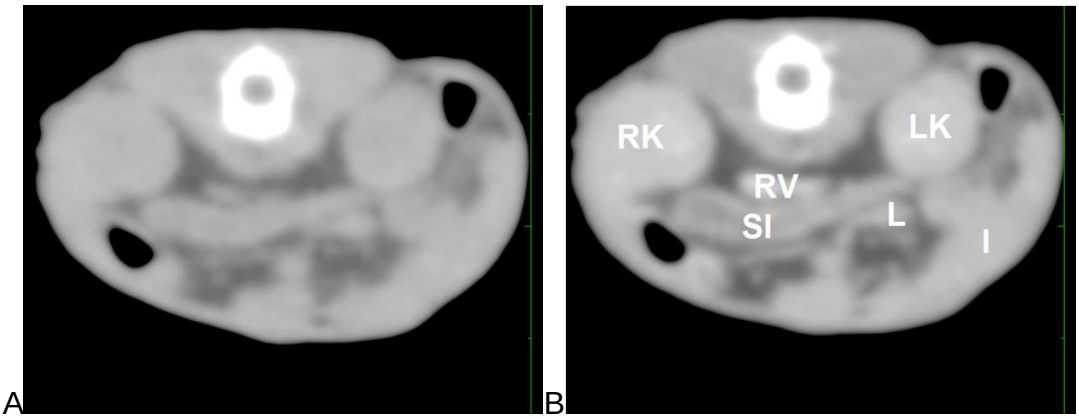

Fig. 9: Transverse CT images of a 16-month-old male marmoset illustrating contrast uptake of the small intestinal walls at the level of L1-2. Dorsal is on top and right on the left of the image. (A) Pre- and (B) post-contrast images displayed in a soft tissue window (WL = 50 and WW = 600). RK = right kidney. LK = left kidney. RV = renal vein. SI = small intestine. I = conglomerate of collapsed intestine. L = lymph node.

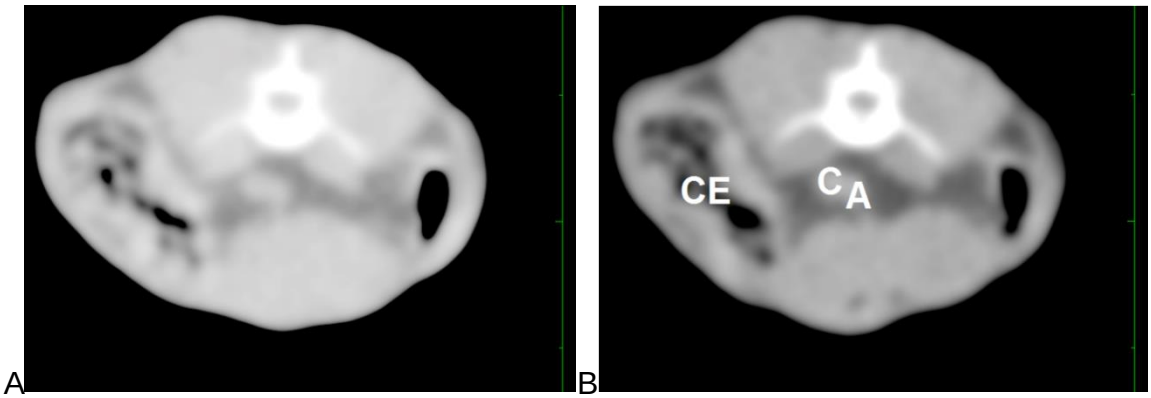

Fig. 10: Transverse CT images of the cecum (CE) of a 12-month-old male marmoset at the level of L5. Dorsal is on top and right on the left of the image. (A) Pre- and (B) post-contrast images displayed in a soft tissue window (WL = 50 and WW = 600). C = Caudal vena cava. A = Aorta.

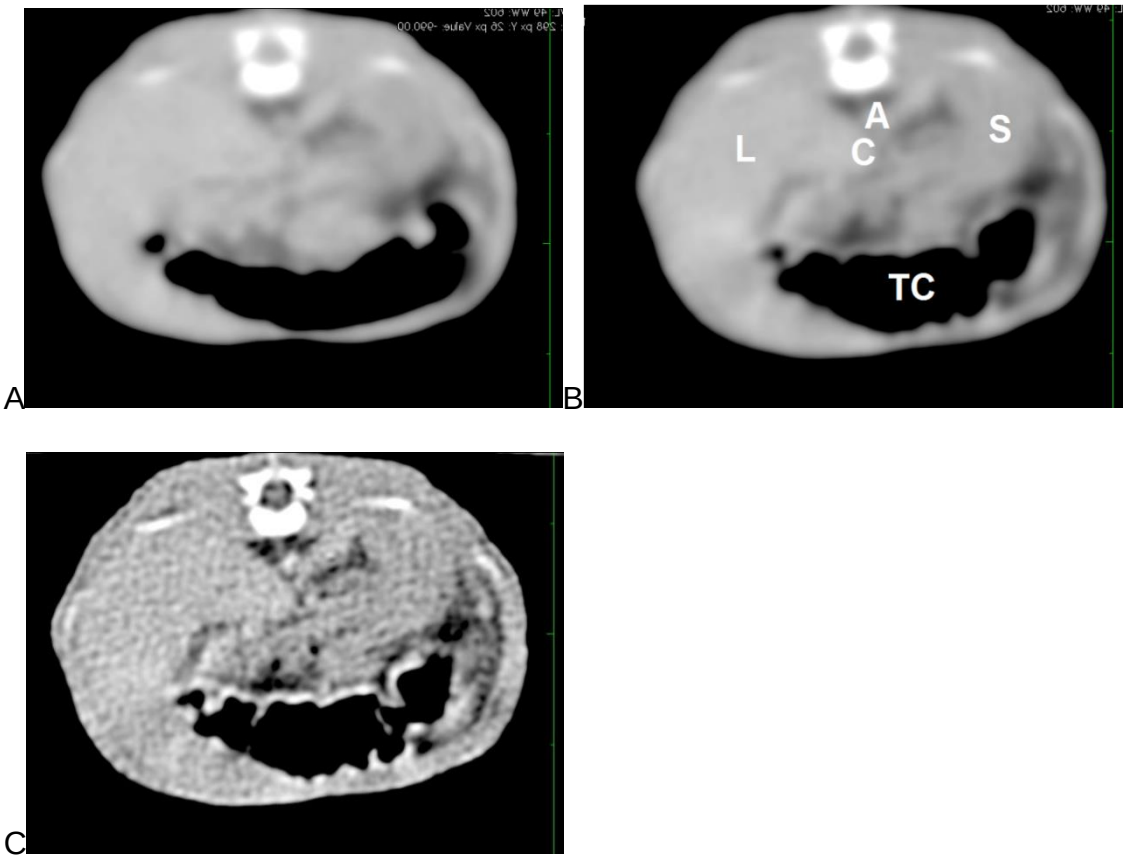

Fig. 11: Transverse CT images of the transverse colon (TC) of a 12-month-old male marmoset at the level of T12-L1. Dorsal is on top and right on the left of the image. (A) Pre- and (B) post-contrast images displayed in a soft tissue window (WL = 50 HU and WW = 600 HU). (C) Post-contrast image using a high frequency algorithm with edge enhancement (WL = 50 HU and WW = 600 HU). A = Aorta. C = caudal vena cava. S = Stomach. L = Liver.

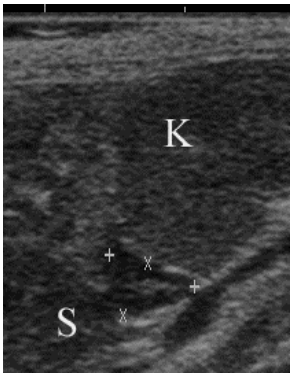

Fig. 12: Sagittal sonogram of the left adrenal gland (indicated by callipers) of a 3-year-old female marmoset. The corticomedullary distinction is clearly visible with a hypoechoic cortex and hyperechoic medulla. The caudally adjacent left kidney (K) shows poor corticomedullary distinction. Note that the spleen (S) is hypoechoic to the kidney and dorsally positioned. Reprint with permission from Veterinary Radiology & Ultrasound.

Fig. 13: Contrary to dogs and cats, exotic animals are often anaesthetized for ultrasonographic examinations. The abdomen should be clipped up to the xiphoid process, including the corresponding intercostal spaces on either side. Due to the high metabolic rate, the animal should be positioned on a heating pad and warmed US gel should ideally be used.

CHAPTER 6

6. GENERAL DISCUSSION AND CONCLUSIONS

This study provided a detailed anatomical description of the thorax and abdomen in clinically healthy marmosets by means of CT. Diagnostic quality images could be obtained in the common marmoset despite its small size and high respiration rate using a dual slice CT scanner. Motion artifacts did occur and influenced the quality of some images. Use of newer generation multi-slice CT scanners would further optimize imaging, and are becoming more readily available in private practice. Therefore, CT examinations of marmosets in a clinical set-up are feasible. Since this study provided a description and reference values for the corresponding normal CT anatomy, it is anticipated that diagnostic proficiency will be facilitated.

The thorough anatomy review in the literature provided the foundation for identification of CT anatomy. Imaging findings differed from described anatomical findings (such as positioning of kidneys in relationship to lumbar vertebrae) and could either be due to different study population, imply more mobility of kidneys similar to cats, or emphasize that CT might be better for certain aspects of anatomic descriptions than actual anatomy studies,[43] since it is done in vivo versus the traditional post-mortem approach. This might be even more valid for dynamic organ systems such as the digestive and the vascular system. This study also emphasized that certain aspects of the skeletal system (such as ribs

or vertebrae number) could be potentially easily incorrectly recorded using radiography in contrast to CT. Use of multi-slice CT scanners would improve 3D reconstructions and enable even more detailed comparison with anatomy.

Exotic animals are being imaged more and more regularly via CT. However, due to their size and species specific anatomy (also reflected in their different normal range of HU of individual organs), standard small animal CT protocols need to be critically assessed and adapted. This study provided recommendations concerning the CT protocol for the common marmoset including different window levels for the abdominal and thoracic cavity.

It must also be remembered that whole body imaging is classically done for smaller exotics and all imaging is done under anesthesia. Dorsal recumbency should be considered for both thoracic and abdominal imaging, if not clinically contraindicated.

A high frequency algorithm ("inner ear algorithm") should be added to the protocol. This algorithm was considered to be particular useful for the thoracic cavity, and to a lesser extend for the abdominal cavity. The inherent edge enhancement of this algorithm enhanced visibility particularly of smaller structures (such as the ureters) and gave more detailed information concerning finer structures. This algorithm also provided similar information than the bone window concerning the skeletal system.

The mean densitometric CT values of the common marmoset for individual abdominal and thoracic organs differed from small animals and emphasized the importance to establish normal reference ranges for different species. Caution

has to be used when applying the provided HUs to other CT machines, since currently accepted standards in medical diagnostics do not call for calibrated HU for comparison. Furthermore the higher HU of abdominal and thoracic organs in comparison to small animals, need to be reflected in higher window levels. Using the provided reference ranges the window level can be even further adapted to organs of interest. Additional windows as described for small animals such as mediastinal windows or for assessment of the urinary system did not result in improvement or additional information.

It needs to be emphasized that the proposed protocol of this study should be seen as a recommendation, since ideal window settings are subjective and may need to be adjusted.

Traditional measurements to reduce motion artifacts such as hyperventilation, positive-pressure ventilation or other breath hold technique can be attempted, however might not prove as successful in small exotics. If the focus is on the thoracic cavity, changing from a whole body scan to a thoracic scan with caudocranial scan direction should be considered.

Motion artifact did not influence the abdomen as much, since a whole body scan used a craniocaudal scan direction already. Due to the small size and the limited resolution of dual slice CT scanners, interpretation of pre-contrast abdominal CT images of the common marmoset were challenging and limited, and i.v. contrast improved the adequate identification and interpretation of the abdomen significantly including examiner confidence level. It must be remembered that i.v. catheter placement can be difficult and time consuming. Post-contrast 3D CT

reconstructions were considered particularly helpful for vascular evaluation, but also assisted with overall anatomical identification and topographic understanding.

Since exotics are anesthetized for all imaging procedures, factors such as reduced patient compliance as with acute abdomen do not influence the choice of imaging modalities. Due to high metabolic rate, warmed up US gel and a heat pad should be used to avoid further compromise of the patient. Possibility of CT-guided biopsy, overcoming superimposition and better soft tissue differentiation to name just a few were advantages of CT over radiography. Gravity dependent atelectasis seemed to influence the HU of the lung. Therefore location of measurement, positioning, duration of positioning, anesthesia protocol and the respiration cycle have to be taken into consideration when assessing the HU of different lung areas.

Depending on the clinical presentation, US and radiography traditionally constitute the modalities of choice for abdominal imaging in small animal patients, with certain examiner and institute preference for the first choice modality. In recent human literature however standard approaches have been questioned in certain clinical applications,[71,72] leading to CT as a first choice imaging modality in humans with acute abdomen for example. In line with similar studies in small animals[69,73-82] different reasonable abdominal imaging modalities were compared in the common marmoset. Since a whole body imaging approach is used for exotics, CT and radiography have the advantage of detecting extra-abdominal lesions (particularly thoracic and skeletal disease) which would be

missed by abdominal US. However, additional thoracic or skeletal imaging could be performed if clinically indicated (and known).

In comparison to small animals the limitations of abdominal radiography were accentuated in the common marmoset by the generally poor serosal abdominal detail, which should not be misinterpreted as ascites. It also resulted in non-visualization of organs such as the spleen and urinary bladder using radiography, which are normally visible in small animals. It was interesting that the abdominal serosal detail was good in the same animals (3/3) on CT.

Based on clinical experience and newer literature, US is often considered the imaging modality of choice for evaluating small animal patients with abdominal disease.[83,84] The adrenal glands served as an excellent example for the benefit of US over CT for the abdomen in the common marmoset. Both on US[38] and CT the adrenal glands were very easily detectable in all common marmosets without a landmark approach unlike in small animals. However US provided additionally good corticomedullary distinction contrary to CT (even on post-contrast images). Additionally, US is a dynamic modality with all its advantages enabling US guided fine needle aspirates, Doppler investigations etc. It should also kept in mind that pregnancy is a contra-indication for CT and since common marmosets are commonly kept for breeding purposes reproductive issues are common clinical presentations. Further clinical studies would be beneficial to assess the benefits of the different imaging modalities in clinical cases and specific diseases in the common marmoset. In summary, this study provided a description and reference values for the thoracic and abdominal CT anatomy in the clinically normal

common marmoset, including recommendations for adapted CT protocols. This baseline study should facilitate CT examinations of marmosets in a clinical set-up and it is anticipated that diagnostic proficiency will be facilitated. Since the imaging decision is multi-factorial and highly dependent on individual case scenario, variables such as cost, time, experience of modality and species, emotional value, availability and accessibility of equipment will be important decision criteria in real case scenarios and realistic clinical settings. Under ideal circumstances US is recommended as the screening tool of choice for the abdomen in the common marmoset, with CT (combined with i.v. contrast) being considered in cases when further diagnostic work-up is required. However, radiography will still play an important role as baseline imaging modality concerning the abdomen - particularly since done as whole body radiograph in the common marmoset - providing simultaneous information about the thorax and the skeletal system. However its limitations must be remembered.

REFERENCES

1. Kishi N, Sato K, Sasaki E, Okano H. Common marmoset as a new model animal for neuroscience research and genome editing technology. *Development, Growth & Differentiation*. 2014;**56**: 53-62.

2. Okano H, Hikishima K, Iriki A, Sasaki E. The common marmoset as a novel animal model system for biomedical and neuroscience research applications. *Seminars in Fetal & Neonatal Medicine*. 2012;**17**: 336-340.

3. Lever MS, Stagg AJ, Nelson M, Pearce P, Stevens DJ, Scott EA, et al. Experimental respiratory anthrax infection in the common marmoset (*Callithrix jacchus*). *International Journal of Experimental Pathology*. 2008;**89**: 171-179.

4. Nelson M, Loveday M. Exploring the innate immunological response of an alternative nonhuman primate model of infectious disease; the common marmoset. *Journal of Immunology Research*. 2014;**2014**: 913632.

5. Nassar-Montoya F, Sainsbury AW, Kirkwood JK, du Boulay GH. Age determination of common marmosets (*Callithrix jacchus*) by radiographic examination of skeletal development. *Journal of Medical Primatology*. 1992;**21**: 259-264.

6. Schultea TD, Smallwood JE, Stott GG. Radiographic evaluation of appendicular skeletal maturation in the common marmoset (*Callithrix jacchus*). *Journal of Medical Primatology*. 1983;**12**: 8-29.

7. Grohmann J, Kuehnel F, Buchwald U, Koeller G, Habla C, Einspanier A. Analysis of the bone metabolism by quantitative computer tomography and

clinical chemistry in a primate model (*Callithrix jacchus*). *Journal of Medical Primatology*. 2012;**41**: 1-10.

8. Grohmann J, Taetzner S, Theuss T, Kuehnel F, Buchwald U, Einspanier A. The conclusiveness of less-invasive imaging techniques (computer tomography, X-ray) with regard to their identification of bone diseases in a primate model (*Callithrix jacchus*). *Journal of Medical Primatology*. 2012;**41**: 130-137.

9. Via LE, Weiner DM, Schimel D, Lin PL, Dayao E, Tankersley SL, et al. Differential virulence and disease progression following Mycobacterium tuberculosis complex infection of the common marmoset (*Callithrix jacchus*). *Infection and Immunity*. 2013;**81**: 2909-2919.

10. Smith TD, Rossie JB, Cooper GM, Schmieg RM, Bonar CJ, Mooney MP, et al. Comparative microcomputed tomography and histological study of maxillary pneumatization in four species of new world monkeys: the perinatal period. *American Journal of Physical Anthropology*. 2011;**144**: 392-410.

11. Bagi CM, Volberg M, Moalli M, Shen V, Olson E, Hanson N, et al. Age-related changes in marmoset trabecular and cortical bone and response to alendronate therapy resemble human bone physiology and architecture. *Anatomical Record*. 2007;**290**: 1005-1016.

12. Johnson LA, Della Santina CC, Wang X. Temporal bone characterization and cochlear implant feasibility in the common marmoset (*Callithrix jacchus*). *Hearing Research*. 2012;**290**: 37-44.

13. Tchirikov M, Schlabritz-Loutsevitch N, Nathanielsz PW, Beindorff N, Schroder HJ. Ductus venosus shunting in marmoset and baboon fetuses. *Ultrasound in Obstetrics & Gynecology*. 2005;**26**: 252-257.

14. Einspanier A, Lieder K, Bruns A, Husen B, Thole H, Simon C. Induction of endometriosis in the marmoset monkey (*Callithrix jacchus*). *Molecular Human Reproduction*. 2006;**12**: 291-299.

15. Hastings JM, Morris KD, Allan D, Wilson H, Millar RP, Fraser HM, et al. Contrast imaging ultrasound detects abnormalities in the marmoset ovary. *American Journal of Primatology*. 2012;**74**: 1088-1096.

16. Ishibashi H, Motohashi HH, Kumon M, Yamamoto K, Okada H, Okada T, et al. Ultrasound-guided non-surgical embryo collection in the common marmoset. *Reproductive Biology*. 2013;**13**: 139-144.

17. Tardif SD, Jaquish CE, Toal RL, Layne DG, Power RA. Estimation of gestational ages in the common marmoset (*Callithrix jacchus*) from published prenatal growth curves. *Journal of Medical Primatology*. 1998;**27**: 28-32.

18. Belcher AM, Yen CC, Stepp H, Gu H, Lu H, Yang Y, et al. Large-scale brain networks in the awake, truly resting marmoset monkey. *The Journal of Neuroscience*. 2013;**33**: 16796-16804.

19. Sawada K, Hikishima K, Murayama AY, Okano HJ, Sasaki E, Okano H. Fetal sulcation and gyrification in common marmosets (*Callithrix jacchus*) obtained by ex vivo magnetic resonance imaging. *Neuroscience*. 2014;**257**: 158-174.

20. Isobe K, Adachi K, Hayashi S, Ito T, Miyoshi A, Kato A, et al. Spontaneous glomerular and tubulointerstitial lesions in common marmosets (*Callithrix jacchus*). *Veterinary Pathology*. 2012;**49**: 839-845.

21. Kaspareit J, Friderichs-Gromoll S, Buse E, Habermann G. Background pathology of the common marmoset (*Callithrix jacchus*) in toxicological studies. *Experimental and Toxicologic Pathology*. 2006;**57**: 405-410.

22. Montali RJ, Bush M. Diseases of the Callitrichidae. In: Fowler M (ed): *Zoo and Wildlife Medicine, 4th ed*. Philadelphia: WB Saunders Company, 1999;369-376.

23. Tucker MJ. A survey of the pathology of marmosets (Callithrix jacchus) under experiment. *Laboratory Animals*. 1984;**18**: 351-358.

24. Wachtman LM, Pistorio AL, Eliades S, Mankowski JL. Calcinosis circumscripta in a common marmoset (*Callithrix jacchus jacchus*). *Journal of the American Association for Laboratory Animal Science*. 2006;**45**: 54-57.

25. Hatt JM, Sainsbury AW. Unusual case of metabolic bone disease in a common marmoset (*Callithrix jacchus*). *The Veterinary Record*. 1998;**143**: 78-80.

26. Bush M, Montali RJ, Kleiman DG, Randolph J, Abramowitz MD, Evans RF. Diagnosis and repair of familial diaphragmatic defects in golden lion tamarins. *Journal of the American Veterinary Medical Association*. 1980;**177**: 858-862.

27. Makungu M, du Plessis WM, Barrows M, Groenewald HB, Koeppel KN. Radiographic thoracic anatomy of the ring-tailed lemur (*Lemur catta*). *Journal of Medical Primatology*. 2014.

28. Young AN, du Plessis WM, Rodriguez D, Beierschmitt A. Thoracic radiographic anatomy in vervet monkeys (*Chlorocebus sabaeus*). *Journal of Medical Primatology*. 2013.

29. Gaschen L, Audet M, Menninger K, Schuurman HJ. Ultrasonographic findings of functioning renal allografts in the cynomolgus monkey (*Macaca fascicularis*). *Journal of Medical Primatology*. 2001;**30**: 46-55.

30. Gaschen L, Kunkler A, Menninger K, Schuurman HJ. Safety of percutaneous ultrasound-guided biopsy of renal allografts in the cynomolgus monkey: results of 348 consecutive biopsies. *Veterinary Radiology & Ultrasound*. 2001;**42**: 259-264.

31. Gaschen L, Menninger K, Schuurman HJ. Ultrasonography of the normal kidney in the cynomolgus monkey (*Macaca fascicularis*): morphologic and Doppler findings. *Journal of Medical Primatology*. 2000;**29**: 76-84.

32. Gaschen L, Schuurman HJ. Ultrasound detection of non-Hodgkin's lymphoma in three cynomolgus monkeys after renal transplantation and cyclosporine immunosuppression. *Journal of Medical Primatology*. 2001;**30**: 88-93.

33. Gaschen L, Schuurman HJ. Contribution of power Doppler sonography to the detection of renal allograft rejection in the cynomolgus monkey. *Investigative Radiology*. 2001;**36**: 335-340.

34. Gaschen L, Schuurman HJ. Renal allograft vasculopathy: ultrasound findings in a non-human primate model of chronic rejection. *The British Journal of Radiology*. 2001;**74**: 411-419.

35. van Diepen HA, Pansier J, Oude Wesselink P, van Drie A, van Duin M, Mulders S. Non-invasive translational Cynomolgus model for studying folliculogenesis and ovulation using color Doppler ultrasonography. *Journal of Medical Primatology*. 2012;**41**: 18-23.

36. Amory JT, du Plessis WM, Beierschmitt A, Beeler-Marfisi J, Palmour RM, Beths T. Abdominal ultrasonography of the normal St. Kitts vervet monkey (*Chlorocebus sabaeus*). *Journal of Medical Primatology*. 2013;**42**: 28-38.

37. James AE, Jr., Brayton JB, Novak G, Wight D, Shehan TK, Bush RM, et al. The use of diagnostic ultrasound in evaluation of the abdomen in primates with emphasis on the rhesus monkey (*Macaca mulatta*). *Journal of Medical Primatology*. 1976;**5**: 160-175.

38. Wagner WM, Kirberger RM. Transcutaneous ultrasonography of the abdomen in the normal common marmoset (*Callithrix jacchus*). *Veterinary Radiology & Ultrasound*. 2005;**46**: 251-258.

39. Wagner WM, Kirberger RM. Radiographic anatomy of the thorax and abdomen of the common marmoset (*Callithrix jacchus*). *Veterinary Radiology & Ultrasound*. 2005;**46**: 217-224.

40. Rylands AB, Mittermeier RA, de Oliveira MM, Kierulff MCM. *Callithrix jacchus. The IUCN Red List of Threatened Species*, 2008. Version 2014.3. <www.iucnredlist.org>. Downloaded on **03 February 2015**.

41. Ludlage E, Mansfield K. Clinical care and diseases of the common marmoset (*Callithrix jacchus*). *Comparative Medicine*. 2003;**53**: 369-382.

42. Consortium. MGSaA. The common marmoset genome provides insight into primate biology and evolution. *Nature genetics*. 2014;**46**: 850-857.

43. Beattie J. The Anatomy of the Common Marmoset (*Hapale jacchus Kuhl*). *Proceedings of the Zoological Society in London*, 1927;593-718.

44. Hill WC. *Primates. Comparative anatomy and toxonomy. Pithecoidea. Platyrrhini (Families Hapalidae and Callimiconidae)*. Edinburgh: University Press, 1957.

45. Barbier A, Bachofen H. The lung of the marmoset (Callithrix jacchus): ultrastructure and morphometric data. *Respiration Physiology*. 2000;**120**: 167-177.

46. Surribas JF, von Lawzewitsch I. The respiratory system of the genus *Callithrix*, the South American monkey. *Primates*. 1987;**28**: 393-402.

47. Casteleyn C, Bakker J, Breugelmans S, Kondova I, Saunders J, Langermans JA, et al. Anatomical description and morphometry of the skeleton of the common marmoset (Callithrix jacchus). *Laboratory Animals*. 2012;**46**: 152-163.

48. Ankel-Simons F. *Primate Anatomy, 3rd ed*. London: Elsevier Academic Press, 2007.

49. Senos R, Benedicto HG, del Rio do Valle CM, del Rio do Valle R, Nayudu PL, Kfoury Junior JR *et al*. *Folia Morphologica*. 2014;**73**: 37-41.

50. Pattison JC, Abbott DH, Saltzman W, Conley AJ, Bird IM. Plasticity of the zona reticularis in the adult marmoset adrenal cortex: voyages of discovery in the New World. *The Journal of Endocrinology*. 2009;**203**: 313-326.

51. Abbott DH, Bird IM. Nonhuman primates as models for human adrenal androgen production: function and dysfunction. *Reviews in Endocrine & Metabolic Disorders*. 2009;**10**: 33-42.

52. Miraglia T, Sadigursky M, Roters FA, Pinto G. Histochemical studies on the adrenal glands of the marmosets (*Callithrix jacchus and Callithrix penicillata*). *Acta Anatomica*. 1976;**94**: 237-247.

53. Miraglia T, Telles Filho M, Branco AL. The male reproductive system of the common marmoset (Callithrix jacchus). *Acta Anatomica*. 1970;**76**: 594-611.

54. Mubiru JN, Hubbard GB, Dick EJ, Jr., Furman J, Troyer DA, Rogers J. Nonhuman primates as models for studies of prostate specific antigen and prostatic diseases. *The Prostate*. 2008;**68**: 1546-1554.

55. Cui KH, Matthews CD. Anatomy of adult female common marmoset (Callithrix jacchus) reproductive system. *Journal of Anatomy*. 1994;**185 (Pt 3)**: 481-486.

56. Stickle RL, Hathcock JT. Interpretation of computed tomographic images. *The Veterinary Clinics of North America Small Animal Practice*. 1993;**23**: 417-435.

57. Prather AB, Berry CR, Thrall DE. Use of radiography in combination with computed tomography for the assessment of noncardiac thoracic disease in the dog and cat. *Veterinary Radiology & Ultrasound*. 2005;**46**: 114-121.

58. Henninger W. Use of computed tomography in the diseased feline thorax. *The Journal of Small Animal Practice*. 2003;**44**: 56-64.

59. De Rycke LM, Gielen IM, Simoens PJ, van Bree H. Computed tomography and cross-sectional anatomy of the thorax in clinically normal dogs. *American Journal of Veterinary Research*. 2005;**66**: 512-524.

60. Rivero MA, Ramirez JA, Vazquez JM, Gil F, Ramirez G, Arencibia A. Normal anatomical imaging of the thorax in three dogs: computed tomography and macroscopic cross sections with vascular injection. *Anatomia, Histologia, Embryologia*. 2005;**34**: 215-219.

61. Ohlerth S, Becker-Birck M, Augsburger H, Jud R, Makara M, Braun U. Computed tomography measurements of thoracic structures in 26 clinically normal goats. *Research in Veterinary Science*. 2012;**92**: 7-12.

62. Cooley SD, Schlipf JW, Jr., Stieger-Vanegas SM. Computed tomographic characterization of the pulmonary system in clinically normal alpacas. *American Journal of Veterinary Research*. 2013;**74**: 572-578.

63. Samii VF, Biller DS, Koblik PD. Normal cross-sectional anatomy of the feline thorax and abdomen: comparison of computed tomography and cadaver anatomy. *Veterinary Radiology & Ultrasound*. 1998;**39**: 504-511.

64. Teixeira M, Gil F, Vazquez JM, Cardoso L, Arencibia A, Ramirez-Zarzosa G, et al. Helical computed tomographic anatomy of the canine abdomen. *Veterinary Journal*. 2007;**174**: 133-138.

65. Rivero MA, Vazquez JM, Gil F, Ramirez JA, Vilar JM, De Miguel A, et al. CT-soft tissue window of the cranial abdomen in clinically normal dogs: an anatomical description using macroscopic cross-sections with vascular injection. *Anatomia, Histologia, Embryologia*. 2009;**38**: 18-22.

66. Zotti A, Banzato T, Cozzi B. Cross-sectional anatomy of the rabbit neck and trunk: comparison of computed tomography and cadaver anatomy. *Research in Veterinary Science*. 2009;**87**: 171-176.

67. Stieger-Vanegas SM, Cebra CK. Contrast-enhanced computed tomography of the gastrointestinal tract in clinically normal alpacas and llamas. *Journal of the American Veterinary Medical Association*. 2013;**242**: 254-260.

68. Beukers M, Grosso FV, Voorhout G. Computed tomographic characteristics of presumed normal canine abdominal lymph nodes. *Veterinary Radiology & Ultrasound*. 2013;**54**:610-617.

69. Fields EL, Robertson ID, Osborne JA, Brown JC, Jr. Comparison of abdominal computed tomography and abdominal ultrasound in sedated dogs. *Veterinary Radiology & Ultrasound*. 2012;**53**: 513-517.

70. Suran JN, Wyre NR. Imaging findings in 14 domestic ferrets (*Mustela putorius furo*) with lymphoma. *Veterinary Radiology & Ultrasound*. 2013;**54**: 522-531.

71. Kellow ZS, MacInnes M, Kurzencwyg D, Rawal S, Jaffer R, Kovacina B, et al. The role of abdominal radiography in the evaluation of the nontrauma emergency patient. *Radiology*. 2008;**248**: 887-893.

72. van Randen A, Lameris W, Luitse JS, Gorzeman M, Hesselink EJ, Dolmans DE, et al. The role of plain radiographs in patients with acute abdominal pain at the ED. *The American Journal of Emergency Medicine*. 2011;**29**: 582-589 e582.

73. Shanaman MM, Schwarz T, Gal A, O'Brien RT. Comparison between survey radiography, B-Mode ultrasonography, contrast-enhanced ultrasonography and contrast-enhanced multi-detector computed tomography findings in dogs with acute abdominal signs. *Veterinary Radiology & Ultrasound*. 2013;**5**4:591-604.

74. Taeymans O, Penninck DG, Peters RM. Comparison between clinical, ultrasound, CT, MRI, and pathology findings in dogs presented for suspected thyroid carcinoma. *Veterinary radiology & ultrasound*. 2013;**54**: 61-70.

75. Alexander K, Joly H, Blond L, D'Anjou MA, Nadeau ME, Olive J, et al. A comparison of computed tomography, computed radiography, and film-screen radiography for the detection of canine pulmonary nodules. *Veterinary Radiology & Ultrasound*. 2012;**53**: 258-265.

76. Byl KM, Kruger JM, Kinns J, Nelson NC, Hauptman JG, Johnson CA. In vitro comparison of plain radiography, double-contrast cystography, ultrasonography, and computed tomography for estimation of cystolith size. *American Journal of Veterinary Research*. 2010;**71**: 374-380.

77. Ober CP, Jones JC, Larson MM, Lanz OI, Werre SR. Comparison of ultrasound, computed tomography, and magnetic resonance imaging in detection of acute wooden foreign bodies in the canine manus. *Veterinary Radiology & Ultrasound*. 2008;**49**: 411-418.

78. Marolf A, Blaik M, Ackerman N, Watson E, Gibson N, Thompson M. Comparison of computed radiography and conventional radiography in detection

of small volume pneumoperitoneum. *Veterinary Radiology & Ultrasound*. 2008;**49**: 227-232.

79. Esterline ML, Radlinsky MG, Biller DS, Mason DE, Roush JK, Cash WC. Comparison of radiographic and computed tomography lymphangiography for identification of the canine thoracic duct. *Veterinary Radiology & Ultrasound*. 2005;**46**: 391-395.

80. Nemanic S, Nelson NC. Ultrasonography and noncontrast computed tomography of medial retropharyngeal lymph nodes in healthy cats. *American Journal of Veterinary Research*. 2012;**73**: 1377-1385.

81. Saunders JH, van Bree H. Comparison of radiography and computed tomography for the diagnosis of canine nasal aspergillosis. *Veterinary Radiology & Ultrasound*. 2003;**44**: 414-419.

82. Robben JH, Pollak YW, Kirpensteijn J, Boroffka SA, van den Ingh TS, Teske E, et al. Comparison of ultrasonography, computed tomography, and single-photon emission computed tomography for the detection and localization of canine insulinoma. *Journal of Veterinary Internal Medicine*. 2005;**19**: 15-22.

83. Sharma A, Thompson MS, Scrivani PV, Dykes NL, Yeager AE, Freer SR, et al. Comparison of radiography and ultrasonography for diagnosing small-intestinal mechanical obstruction in vomiting dogs. *Veterinary Radiology & Ultrasound*. 2011;**52**: 248-255.

84. Tyrrell D, Beck C. Survey of the use of radiography vs. ultrasonography in the investigation of gastrointestinal foreign bodies in small animals. *Veterinary Radiology & Ultrasound*. 2006;**47**: 404-408.